Ⅳ．研究成果の刊行物・別刷

JOURNAL OF VIROLOGY, Oct. 2009, p. 9993–10006 Vol. 83, No. 19
0022-538X/09/$08.00+0 doi:10.1128/JVI.00509-09

The Hepatitis C Virus Core Protein Contains a BH3 Domain That Regulates Apoptosis through Specific Interaction with Human Mcl-1▽†

Nur Khairiah Mohd-Ismail,[1,2] Lin Deng,[3] Sunil Kumar Sukumaran,[4] Victor C. Yu,[4,5] Hak Hotta,[3] and Yee-Joo Tan[1]*

Collaborative Anti-Viral Research Group, Institute of Molecular and Cell Biology, Singapore[1]; NUS Graduate School for Integrative Sciences and Engineering, Singapore[2]; Division of Microbiology, Kobe University Graduate School of Medicine, Kobe, Japan[3]; Mechanisms of Apoptosis in Mammalian Cell Group, Institute of Molecular and Cell Biology, Singapore[4]; and Department of Pharmacy, Faculty of Science, National University of Singapore, Singapore[5]

Received 11 March 2009/Accepted 8 July 2009

The hepatitis C virus (HCV) core protein is known to modulate apoptosis and contribute to viral replication and pathogenesis. In this study, we have identified a Bcl-2 homology 3 (BH3) domain in the core protein that is essential for its proapoptotic property. Coimmunoprecipitation experiments showed that the core protein interacts specifically with the human myeloid cell factor 1 (Mcl-1), a prosurvival member of the Bcl-2 family, but not with other prosurvival members (Bcl-X_L and Bcl-w). Moreover, the overexpression of Mcl-1 protects against core-induced apoptosis. By using peptide mimetics, core was found to release cytochrome *c* from isolated mitochondria when complemented with Bad. Thus, core is a bona fide BH3-only protein having properties similar to those of Noxa, a BH3-only member of the Bcl-2 family that binds preferentially to Mcl-1. There are three critical hydrophobic residues in the BH3 domain of the core protein, and they are essential for the proapoptotic property of the core protein. Furthermore, the genotype 1b core protein is more effective than the genotype 2a core protein in inducing apoptosis due to a single-amino-acid difference at one of these hydrophobic residues (residue 119). Replacing this residue in the J6/JFH-1 infectious clone (genotype 2a) with the corresponding amino acid in the genotype 1b core protein produced a mutant virus, J6/JFH-1(V119L), which induced significantly higher levels of apoptosis in the infected cells than the parental J6/JFH-1 virus. Furthermore, the core protein of J6/JFH-1(V119L), but not that of J6/JFH-1, interacted with Mcl-1 in virus-infected cells. Taken together, the core protein is a novel BH3-only viral homologue that contributes to the induction of apoptosis during HCV infection.

Hepatitis C virus (HCV), a positive-stranded RNA virus of the family *Flaviviridae*, is the major cause of non-A, non-B hepatitis worldwide. The HCV genome encodes a precursor polyprotein of ~3,000 amino acids (aa) that is processed cotranslationally and posttranslationally to give rise to viral structural and nonstructural proteins (2). The core protein is encoded by the N-terminal portion of the HCV precursor polyprotein and cleaved from the polyprotein by cellular signal peptidase to give the immature form of the core protein (aa 1 to 191). This then is further cleaved by membrane-associated signal peptide peptidase to give the mature core protein, whose C terminus is not precisely known but lies between residues 170 and 179 (see reviews in references 33, 42, and 52). The mature core protein is thought to constitute the HCV capsid and is the predominant form detected in virus particles purified from the sera of patients with chronic HCV infection (42, 74). A recent paper also reported that the maturation of the core protein is required for the production of HCV using the JFH-1 infectious clone (65).

Besides its role in the encapsidation of viral RNA, the core protein has been found to interfere with many cellular pathways, including cell signaling, transcriptional activation, lipid metabolism, carcinogenesis, and apoptosis (see reviews in references 33, 42, and 52). As the regulation of apoptosis during viral infection is an important determinant in the struggle between virus and host for survival, many viruses encode viral proteins that can regulate apoptosis in the infected host cells and manipulate this process to their advantage. In the case of HCV, the mechanisms by which the virus maintains viral persistence and promotes hepatocellular carcinoma are not well understood, but several HCV proteins have the ability to modulate apoptosis (see recent reviews in references 20 and 28). In particular, the core protein has been shown to modulate apoptosis, and it seems that the core protein can inhibit as well as promote apoptosis, depending on the death stimuli and types of cells used (3, 9, 13, 25, 36, 40, 49, 53, 54, 57, 60, 76).

In this study, we characterized one of the mechanisms by which the mature form of the core protein from a genotype 1b strain induces apoptosis in Huh7 cells. Following the experimental designs used in previous studies (29, 38, 40, 55, 72), the mature form of the core protein is assumed to be constituted by residues 1 to 173 of the HCV precursor polyprotein, and

* Corresponding author. Mailing address: Cancer and Developmental Cell Biology Division, Institute of Molecular and Cell Biology, 61 Biopolis Drive, A*STAR (Agency for Science, Technology and Research), Biopolis, Singapore 136873, Singapore. Phone: 65-65869625. Fax: 65-67791117. E-mail: mcbtanyj@imcb.a-star.edu.sg.

† Supplemental material for this article may be found at http://jvi.asm.org/.

▽ Published ahead of print on 15 July 2009.

this shall be referred to as the core protein in this study. Here, we demonstrate that the core protein contains a functional Bcl-2 homology 3 (BH3) domain that is essential for its proapoptotic property and ability to interact with human myeloid cell factor 1 (Mcl-1), a prosurvival member of the Bcl-2 family (31). Detailed molecular analysis and infection studies using the J6/JFH-1 infectious clone showed that the core protein is a bona fide BH3-only protein that contributes to the induction of apoptosis during HCV infection by mimicking Noxa and interfering with the prosurvival function of Mcl-1.

MATERIALS AND METHODS

Construction of plasmids. Expression plasmids for the wild-type core protein and mutants were generated by PCR using Titanium *Taq* DNA polymerase (Clontech Laboratories Inc., Palo Alto, CA). Two plasmids containing full-length HCV genomes were used as templates. The first one is a 1b strain cloned in Singapore (59), and the second is the JFH-1 clone, which is a 2a strain (68). All sequences were confirmed by sequencing performed by the core facilities at the Institute of Molecular and Cell Biology, Singapore. The pXJ40flag vector is used so that a flag epitope is fused to the N terminus of the core protein, and this allows the comparison of protein expression levels with an anti-flag antibody.

Transient transfections, CaspACE fluorometric assay, and Western blot analysis. Transient transfections of Huh7 cells were performed using Lipofectamine reagent (Invitrogen, Carlsbad, CA) according to the manufacturer's protocol. Approximately 16 h after transfection, the activation of caspase-3 was quantified by using a CaspACE fluorometric assay system from Promega Corporation (Madison, WI) as previously described (63).

Western blot analysis was performed as previously described (64). The primary antibodies (anti-myc monoclonal and anti-myc and anti-Mcl-1 polyclonal [Santa Cruz Biotechnology, Santa Cruz, CA], anti-Mcl-1 monoclonal [Calbiochem, La Jolla, CA], anti-actin monoclonal, anti-Hsp-60 monoclonal, anti-flag monoclonal and polyclonal [Sigma, St. Louis, MO], anti-poly[ADP-ribose] polymerase [PARP] polyclonal [Cell Signaling Technology Inc., Beverly, MA], anti-cytochrome *c* monoclonal [BD PharMingen, BD Biosciences, San Jose, CA], and anti-Noxa [Imgenex, San Diego, CA]) were purchased. Anti-core protein monoclonal antibody (clone 2H9; a kind gift from T. Wakita, Department of Virology II, National Institute of Infectious Diseases, Tokyo, Japan) was used to detect the core protein of HCV (68).

Coimmunoprecipitation experiments. For the coimmunoprecipitation experiments, each 6-cm dish of cells was resuspended in 200 μl of immunoprecipitation (IP) buffer (50 mM Tris-HCl, pH 8, 150 mM NaCl, 0.5% NP-40, 0.5% deoxycholic acid, 0.005% sodium dodecyl sulfate [SDS], and 1 mM phenylmethylsulfonyl fluoride) and subjected to freeze-thawing six times. Anti-flag monoclonal antibody conjugated to Sepharose beads (Sigma) were added to 150 μl of the lysates, and the mixture was subjected to end-over-end mixing at 4°C for 6 h. Beads were washed four times with cold IP buffer, and then 15 μl of Laemmli's SDS buffer was added and the samples were boiled at 100°C for 5 min to release the immunocomplexes. Samples were separated by SDS-polyacrylamide gel electrophoresis and subjected to Western blot analysis.

Alternatively, rabbit anti-Mcl-1 polyclonal antibody was used to immunoprecipitate endogenous Mcl-1 protein. In this case, 7 μg of antibody (either anti-Mcl-1 or anti-hemagglutinin [HA] polyclonal antibody [Santa Cruz Biotechnology]) was added to the lysates obtained from two dishes of cells and allowed to mix for 1 h at room temperature. Protein A agarose beads (Roche, Indianapolis, IN) were added, and the mixture was subjected to end-over-end mixing at 4°C overnight. The coimmunoprecipitated proteins then were detected as described above.

Quantification of autoradiographs. An imaging densitometer (Bio-Rad, Hercules, CA) was used for the quantification of the intensities of specific bands on autoradiographs.

In vitro cytochrome *c* release assay. For the in vitro cytochrome *c* release assays, mitochondria were isolated from 293T cells as previously described (22). Briefly, 293T cells were suspended in isolation buffer (320 mM sucrose, 1 mM EDTA, 50 mM HEPES [pH 7.5]) and disrupted by 25 expulsions through a 27-gauge needle. The disrupted cells were spun at 1,000 × *g* for 10 min to remove cell debris and nuclei. The supernatant was centrifuged at 7,000 × *g* for 10 min, and the pellet was retained as the heavy membrane fraction containing the mitochondria. The mitochondrion-containing pellets then were resuspended in assay buffer (250 mM sucrose, 2 mM KH_2PO_4, 5 mM sodium succinate, 25 mM EGTA, and 10 mM HEPES [pH 7.5]) at 0.5 mg/ml. Equal amounts of mitochondria were treated with the indicated peptides for 30 min at room temperature, followed by centrifugation. Both the supernatant and pellet then were subjected to SDS-polyacrylamide gel electrophoresis, followed by Western blot analysis to determine the amount of cytochrome *c* released from the mitochondria. Hsp-60 was used as a loading control for the pellet.

Synthesis of peptides. A peptide that corresponds to residues 118 to 149 of the genotype 1b core protein (NLGKVIDTLTCGFADLMGYIPLVGAPLGG AAR) was synthesized and purified to 95% purity (Sigma Genosys, Japan). Peptides containing the BH3 domain of Bad (NLWAAQRYGRELRRMSDEF VDSFKK) or Noxa (VPADLKDECAQLRRIGDKVNLRQKL) also were synthesized and purified to 95% purity (Mimotopes, Clayton, Victoria, Australia).

Generation of recombinant HCV. The pFL-J6/JFH-1 plasmid encoding the entire viral genome of a chimeric strain of HCV genotype 2a, J6/JFH-1 (37), was kindly provided by C. M. Rice, Center for the Study of Hepatitis C, The Rockefeller University. To generate mutant virus possessing a core protein mutation, a nucleotide substitution was introduced into pFL-J6/JFH-1 by site-directed mutagenesis using a QuikChange site-directed mutagenesis kit (Stratagene, La Jolla, CA). All PCR-amplified DNA fragments were verified extensively using an ABI PRISM 3100-Avant Genetic Analyzer (Applied Biosystems, Foster City, CA). Each of the plasmids was linearized by XbaI digestion and in vitro transcribed by using T7 RiboMAX (Promega) to generate the full-length viral genomic RNA. The in vitro-transcribed RNA (10 μg) was transfected into Huh7.5 cells by means of electroporation (975 μF, 270 V) using a Gene Pulser (Bio-Rad). The cells then were cultured in complete medium, and the supernatant was propagated as a virus stock. Culture supernatants of uninfected cells served as a control (mock preparation). Virus infectivity was measured by indirect immunofluorescence as previously described (17) and expressed as cell-infecting units (CIU) per milliliter.

Proliferation, caspase-3, and DNA fragmentation assays. Huh7.5 cells were seeded in 96-well plates at a density of 1.0×10^4 cells per well and cultured overnight. The cells then were infected with recombinant HCV at a multiplicity of infection of 0.1 CIU/cell or with a mock preparation. At different time points postinfection (p.i.), cell viabilities were determined by WST-1 proliferation assays (Roche, Mannheim, Germany) as described previously (17, 48).

Caspase-3 and DNA fragmentation assays also were performed on the infected cells as previously described (17).

HCV RNA quantitation. To measure intracellular HCV RNA replication levels, total RNA was extracted from the cells using an RNeasy Mini kit (Qiagen, Valencia, CA) according to the manufacturer's instructions. One microgram of total RNA was reverse transcribed using a QuantiTect reverse transcription kit (Qiagen) with random primers and was subjected to quantitative real-time PCR analysis using SYBR premix Ex *Taq* (Takara Bio, Kyoto, Japan) in a MicroAmp 96-well reaction plate and an ABI PRISM 7000 (Applied Biosystems, Foster, CA). The primers used to amplify an NS5A region of the HCV genome were 5′-AGACGTATTGAGGTCCATGC-3′ (sense) and 5′-CCGCAGCGACGGTG CTGATAG-3′ (antisense). As an internal control, human glyceraldehyde-3-phosphate dehydrogenase expression levels were measured using primers 5′-G CCATCAATGACCCCTTCATT-3′ (sense) and 5′-TCTCGCTCCTGGAAGA TGG-3′ (antisense).

Statistical analysis. Either the two-tailed Student's *t* test or one-way analysis of variance (using SPSS version 16.0) was applied to evaluate the statistical significance of differences measured from the data sets. $P < 0.05$ was considered statistically significant.

RESULTS

A BH3-like domain is present in the core protein. The family of Bcl-2 proteins constitutes one of the biologically important gene products in the regulation of apoptosis (see recent reviews in references 1, 16, 67, and 75). The Bcl-2 proteins may be classified broadly into three classes: prosurvival members containing multiple Bcl-2 homology domains, proapoptotic members containing multiple Bcl-2 homology domains, and proapoptotic members containing the BH3 domain only. The examination of the amino acid sequence of the core protein revealed that there is a BH3-like domain near the C terminus. An alignment of this domain with BH3 domains of the Bcl-2 family of proteins is shown in Fig. 1A. The BH3-like domain of the core protein contains L (residue 119) and D (residue 124)

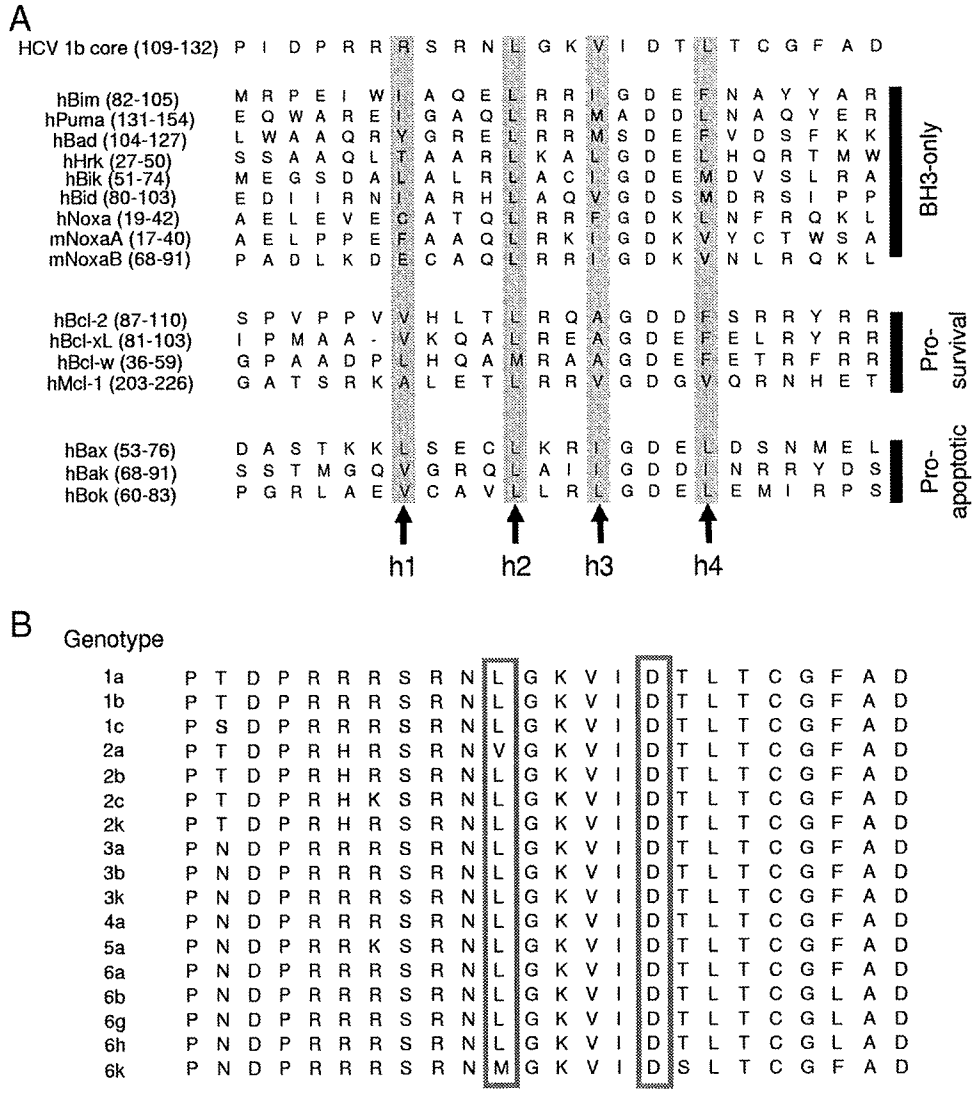

FIG. 1. Identification of a BH3-like domain in the core protein. (A) Alignment of the BH3 domain of the genotype 1b core protein with the BH3 domains of members of the Bcl-2 family. Numbers in parentheses represent the positions of amino acid residues of the respective proteins. The four hydrophobic amino acids that make critical contacts with residues in the BH3 recognition grooves present on the surfaces of the prosurvival Bcl-2 family proteins are indicated as h1 to h4. (B) Alignment of the core protein (residues 109 to 132) of different genotypes. The consensus sequences for these genotypes were obtained from http://hcv.lanl.gov/content/hcv-index. The highly conserved L and D residues, at positions 119 and 124 of the genotype 1b core protein, respectively, in BH3 domains are boxed.

separated by four residues, as in other known BH3 domains. This domain is highly conserved among the major HCV genotypes, with the exception of genotypes 2a and 6k, which have V and M residues at position 119, respectively (Fig. 1B).

The BH3 domain of the core protein is essential for the induction of apoptosis and its interaction with human Mcl-1. The overexpression of the core protein (with a flag epitope at the N terminus) in Huh7 cells, via the transient transfection of a cDNA expression plasmid containing the genotype 1b core protein gene, induced significant levels of apoptosis as determined by the activation of caspase-3, which is a hallmark of apoptosis (Fig. 2A). The deletion of the BH3 domain in the core protein (designated coreΔ115-128aa) abolished its proapoptotic property, indicating that this domain is essential for the induction of apoptosis. Consistently, the cleavage of endogenous PARP, a substrate of activated caspase-3, was clearly observed in Huh7 cells expressing the wild-type core protein but not in those expressing coreΔ115-128aa (Fig. 2B).

To understand how the core protein modulates the function of the Bcl-2 family of proteins, coimmunoprecipitation experiments were performed to determine if the core protein can interact with representative prosurvival members of the Bcl-2 family. As shown in the top panel of Fig. 3A, Mcl-1 was specifically coimmunoprecipitated by the core protein (lane 8) but not by an irrelevant protein, glutathione *S*-transferase (GST) (lane 7). The BH3 domain of the core protein is essential for its interaction with Mcl-1, as coreΔ115-128aa failed to coimmunoprecipitate Mcl-1 (lane 9). These results indicate that the core protein induces apoptosis by interfering directly with the prosurvival function of Mcl-1. In contrast, no significant inter-

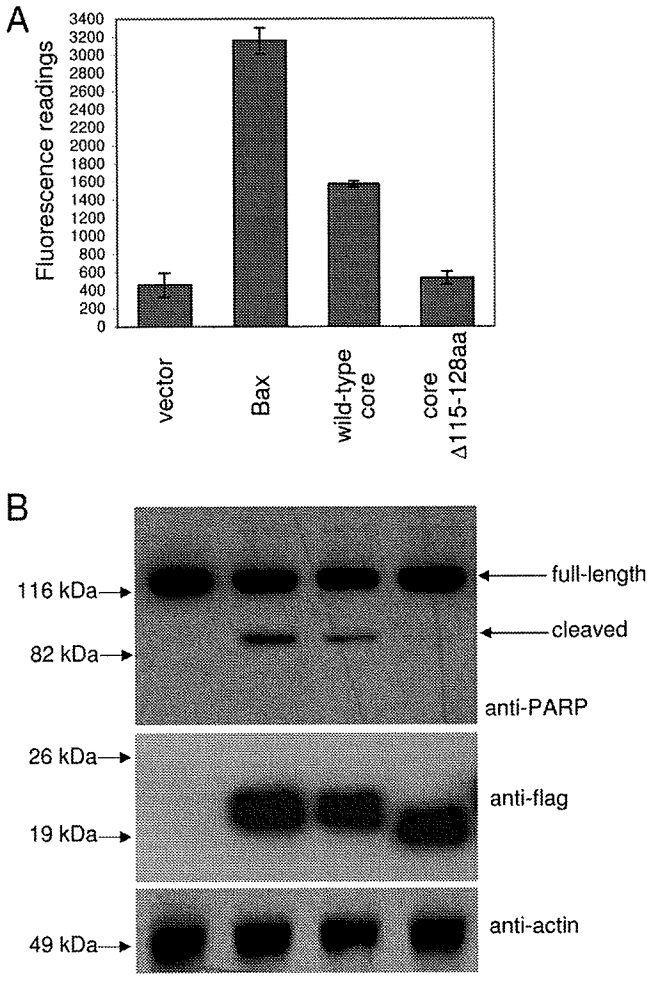

FIG. 2. Induction of apoptosis by the overexpression of the core protein in Huh7 cells. (A) A CaspACE fluorometric assay system from Promega Corporation (Madison, WI) was used to measure the activation of caspase-3, which is a hallmark of apoptosis, in Huh7 cells that were transfected with vector only, a classical apoptosis inducer (Bax), the wild-type core protein, and a core protein mutant lacking the putative BH3 domain (coreΔ115-128aa). All experiments were performed in triplicate, and the average values with standard deviations are plotted. (B) Western blot analysis also was performed to determine the cleavage of endogenous PARP, which is a substrate of activated caspase-3, from 116 to 83 kDa (top). Similarly, the expression levels of the different proteins were determined using anti-flag antibody (middle). The amounts of total cell lysates loaded were verified by measuring the levels of endogenous actin (bottom).

action was observed between the core protein and two other prosurvival proteins, Bcl-X_L and Bcl-w (lanes 1 to 6).

The interaction between the core protein and endogenous Mcl-1 was determined by overexpressing the core protein in Huh7 cells. As shown in Fig. 3B, the core protein was coimmunoprecipitated with endogenous Mcl-1 (lane 3). On the other hand, the core protein was not coimmunoprecipitated when an irrelevant antibody (anti-HA) (lane 4) was used for IP. Consistently with the results in Fig. 3A, only a small amount of coreΔ115-128aa was coimmunoprecipitated with endogenous Mcl-1 (lane 5). To estimate the degree of reduction in the binding of coreΔ115-128aa to endogenous Mcl-1, an imaging densitometer was used to quantify the intensities of specific bands on the autoradiographs obtained in three independent coimmunoprecipitation experiments (see Fig. S1 in the supplemental material). The ratios of signals for the expression of flag-tagged core protein, endogenous Mcl-1, and actin (internal control) all are close to 1 (0.94 to 1.14), indicating that the expression levels of these proteins in the two sets of cells (either transfected with cDNA construct for expressing flag-core or flag-coreΔ115-128aa) were similar. From the three independent experiments, the average amount of coreΔ115-128aa coimmunoprecipitated specifically by the Mcl-1 antibody is 14.2% (± 10.7%) of the amount of wild-type core protein coimmunoprecipitated. This implies that the deletion of the BH3 domain does not completely abolish the interaction between the core protein and endogenous Mcl-1 but reduces the interaction greatly.

Overexpression of Mcl-1 or Bcl-X_L prevents core protein-induced apoptosis. To examine the protective effects of the prosurvival Bcl-2 proteins in Huh7 cells, transfections were performed with plasmids expressing myc-tagged Bcl-2, Bcl-X_L, Bcl-w, or Mcl-1 (Fig. 4A and B). Consistent with studies of other cell lines (12, 66), the transient high-level expression of Bcl-2 also caused apoptosis in Huh7 cells (lane 1). Interestingly, the overexpression of Bcl-w also induced a significant level of apoptosis in Huh7 cells (lane 3), and this phenomenon has not been reported previously. Cells overexpressing Bcl-X_L, but not Mcl-1, also had a slightly higher level of apoptosis than that of the vector control cells (lanes 2 and 4).

Huh7 cells were cotransfected with plasmids for expressing myc-Mcl-1 and flag-core or myc-Bcl-X_L and flag-core. As shown in Fig. 4C and D, the level of apoptosis was significantly reduced in cells expressing both Mcl-1 and the core protein (lane 3) compared to those expressing the core protein only (lane 2). When the same experiment was repeated using Bcl-X_L, the level of apoptosis was reduced to a lesser extent (lane 5). However, this may be due to the low level of apoptosis induced by the overexpression of Bcl-X_L (lane 6). The level of the core protein expressed in the presence of Bcl-X_L also was decreased greatly, but the smaller amount of the core protein expressed still induced a high level of apoptosis (lane 5). However, when a broad caspase inhibitor (z-VAD-fmk) was used, the core protein level in cells coexpressing Bcl-X_L increased (see Fig. S2 in the supplemental material), indicating that the transfection efficiencies were similar in the different samples. To resolve this uncertainty, the experiment was repeated with a smaller amount of Bcl-X_L plasmid (0.5 μg). Under this condition, the overexpression of Bcl-X_L did not induce apoptosis (lane 8), and the level of apoptosis also was reduced in cells expressing both Bcl-X_L and the core protein (lane 7) compared to those expressing the core protein only (lane 2). Thus, the results show that the overexpression of either Mcl-1 or Bcl-X_L protects against core protein-induced apoptosis.

Bad enhances the ability of the core protein to release cytochrome *c* from isolated mitochondria. The ability of a core protein peptide, which contains residues 118 to 149 of the genotype 1b core protein, to release cytochrome *c* from the mitochondria was tested using 293T cells instead of Huh7 cells, as the method for the isolation of mitochondria from 293T cells is well established. The core protein induced apoptosis in 293T cells in the same manner as that in Huh7 cells (see Fig.

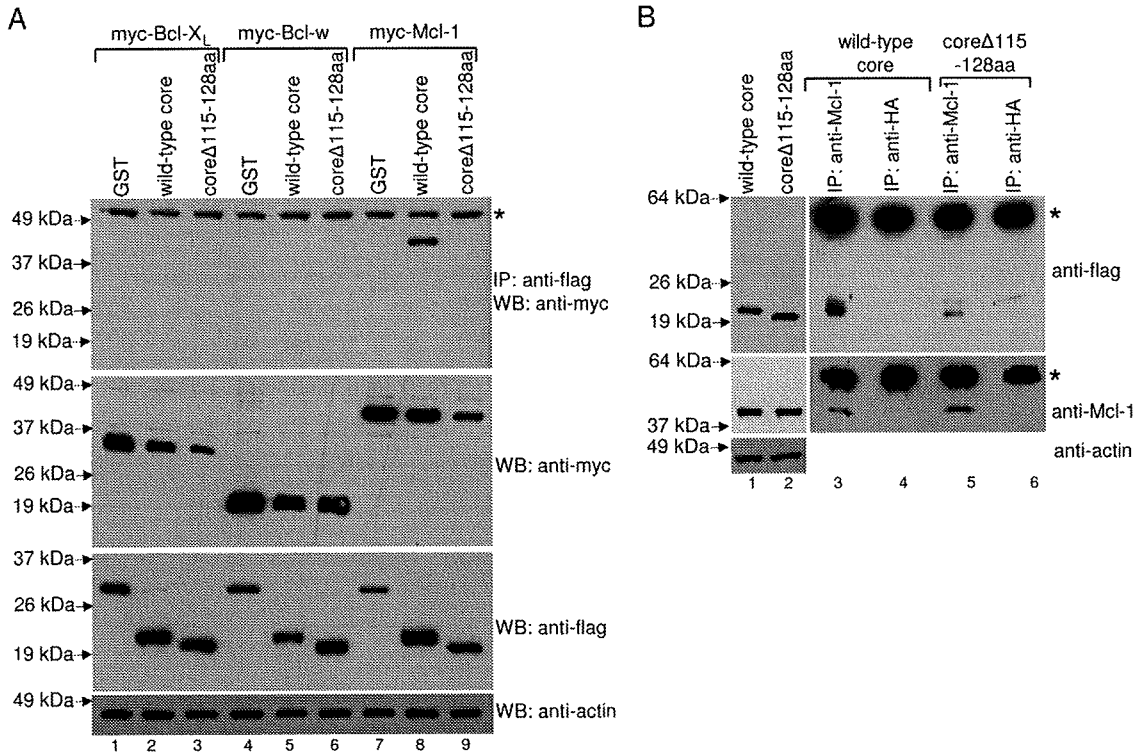

FIG. 3. Interaction of the core protein with prosurvival members of the Bcl-2 family determined by coimmunoprecipitation experiments. (A) Huh7 cells were transfected with cDNA constructs for expressing flag-GST (negative control), flag-core, or flag-coreΔ115-128aa, and myc-tagged prosurvival members of the Bcl-2 family (myc-Bcl-X_L [lanes 1 to 3], myc-Bcl-w [lanes 4 to 6], and myc-Mcl-1 [lanes 7 to 9]). The cells were harvested at ~16 h posttransfection, lysed, and subjected to IP with anti-flag monoclonal antibody conjugated to Sepharose beads. The amount of myc-tagged proteins that coimmunoprecipitated (IP) with the flag-tagged proteins was determined by Western blot analysis (WB) with an anti-myc rabbit polyclonal antibody (top). The amounts of myc-tagged and flag-tagged proteins in the lysates before IP were determined by subjecting aliquots of the lysates to Western blot analysis (middle). The protein marked with an asterisk represents the heavy chain of the antibody used for IP (top), and the amounts of total cell lysates loaded were verified by measuring the levels of endogenous actin (bottom). (B) Huh7 cells were transfected with cDNA constructs for expressing flag-core or flag-coreΔ115-128aa. IP then was performed using anti-Mcl-1 or anti-HA rabbit polyclonal antibodies and protein A agarose beads. The amounts of flag-tagged core protein in the lysates before IP (lanes 1 and 2) or coimmunoprecipitated (lanes 3 to 6) were determined by Western blot analysis with an anti-flag monoclonal antibody (top). Similarly, the amounts of endogenous Mcl-1 in these samples were detected using an anti-Mcl-1 monoclonal antibody (middle). The protein marked with an asterisk represents the heavy chain of the antibody used for IP (top), and the amounts of total cell lysates loaded were verified by measuring the levels of endogenous actin (bottom).

S3 in the supplemental material). As shown in Fig. 5A, both the Bad and core protein peptides were inefficient in inducing the release of cytochrome *c*, as only a small amount of cytochrome *c* was detected in the supernatant from the treated mitochondria when 200 μM of either peptide was used. However, when Bad and core protein peptides were used in combination, the release of cytochrome *c* was observed at the much lower concentration of 50 μM (consisting of 25 μM Bad peptide and 25 μM core protein peptide). Furthermore, the release of cytochrome *c* increased in a dose-dependent manner. The amount of cytochrome *c* left in the treated mitochondria (i.e., pellet) decreased correspondingly, while the amount of control protein, Hsp-60, was not affected.

The same experiment was repeated using the Noxa peptide (Fig. 5B). Consistently with a previous study (11), the Noxa peptide alone was inefficient in inducing the release of cytochrome *c*, but when it was combined with the Bad peptide, the release was significantly enhanced. The peptide(s) dosage required was similar to the amount required for the core protein and Bad, indicating that the complementation between the core protein and Bad is similar to the complementation between Noxa and Bad. In addition, complementation between the core protein and Bad also was observed when they were coexpressed in Huh7 cells (see Fig. S4 in the supplemental material).

The three hydrophobic residues in the BH3 domain of the core protein are important for apoptosis induction. Site-directed mutagenesis and structural studies of the interactions between the prosurvival Bcl-2 proteins and BH3 domains have revealed the mechanism by which BH3 domains are bound to the hydrophobic grooves present on the surfaces of the prosurvival Bcl-2 proteins (see reviews in references 50 and 69). In particular, the BH3 domain usually contains four hydrophobic residues (h1, h2, h3, and h4) (Fig. 1A) that make contacts critical for the stability of the complex. Interestingly, the core protein contains hydrophobic residues at the h2, h3, and h4 positions (Fig. 1A). An alanine substitution experiment was performed to determine if these residues are essential for the proapoptotic property of the core protein (Fig. 6A and B). The results showed that replacement of either L119, V122, or L126

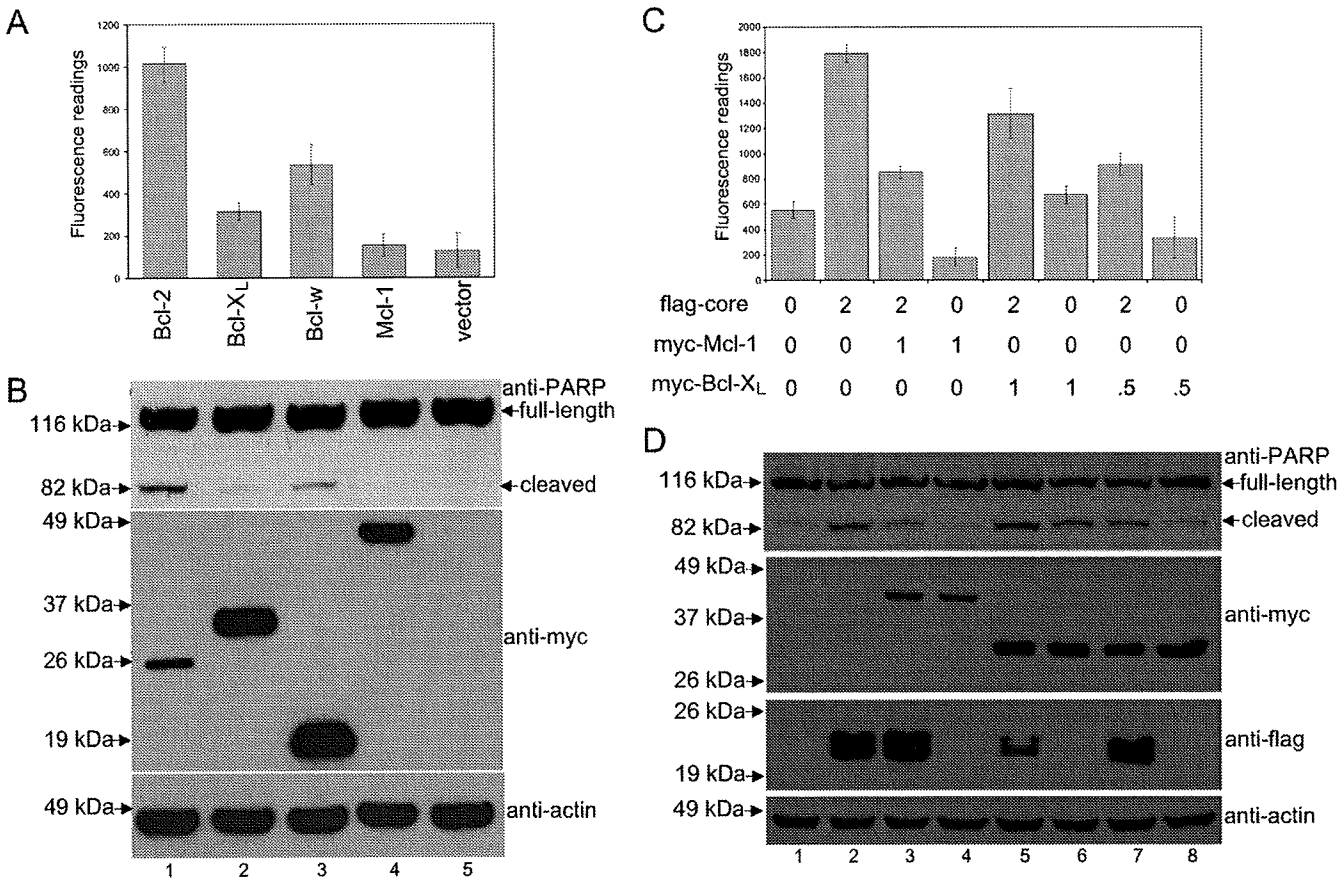

FIG. 4. Effects of Mcl-1 and Bcl-X_L overexpression on the proapoptotic property of the core protein. (A) A CaspACE fluorometric assay system from Promega Corporation (Madison, WI) was used to measure the activation of caspase-3 in Huh7 cells that were transfected with Bcl-2, Bcl-X_L, Bcl-w, Mcl-1, or vector only. All experiments were performed in triplicate, and the average values with standard deviations are plotted. (B) Western blot analysis also was performed to determine the cleavage of endogenous PARP (top) and expression levels of the myc-tagged prosurvival members of the Bcl-2 family (middle). The amounts of total cell lysates loaded were verified by measuring the levels of endogenous actin (bottom). (C) A CaspACE fluorometric assay system from Promega Corporation (Madison, WI) was used to measure the activation of caspase-3 in Huh7 cells that were singly transfected with vector, the wild-type core protein, Mcl-1, or Bcl-X_L, or that were cotransfected with wild-type core protein and Mcl-1 or Bcl-X_L. The amounts of flag-core and myc-Mcl-1 or myc-Bcl-X_L DNAs used in each of the transfections are indicated in micrograms. In each transfection, the total amount of DNA was normalized to 3 μg with the addition of empty vector if necessary. All experiments were performed in triplicate, and the average values with standard deviations are plotted. (D) Western blot analysis also was performed to determine the cleavage of endogenous PARP (top) and expression levels of myc-tagged Mcl-1 and Bcl-X_L and flag-tagged core protein (middle). The amounts of total cell lysates loaded were verified by measuring the levels of endogenous actin (bottom).

with A completely abolishes the proapoptotic property of the core protein. On the other hand, the replacement of the highly conserved D124 residue with A seems to increase the proapoptotic property of the core protein slightly. The levels of activated caspase-3 induced by the wild-type core protein and the D124A substitution mutant in six independent experiments were compared using the two-tailed Student's *t* test, and the difference was found to be statistically significant (Fig. 6C). This phenomenon has not been reported for other BH3-only proteins, but there are a few known functional BH3 domains that do not contain D at this position (54, 55).

Furthermore, coimmunoprecipitation experiments showed that the L119A, V122A, and L126A substitution mutants have reduced binding to Mcl-1 (Fig. 7A). Similar results were obtained in four independent experiments, and the percentages of binding compared to that of the wild-type core protein were estimated by using an imaging densitometer to measure the intensity of the core protein signals after coimmunoprecipitation. For each experiment, three different autoradiographs (with different exposure times) were used, and the average values are shown in Table S1 in the supplemental material. The average percentages in binding of Mcl-1 to the L119A, V122A, and L126A mutants are 33, 62, and 9% of the binding to the wild-type core protein, respectively. For all three mutants, the reduced interactions with Mcl-1 compared to those of the wild-type core protein are statistically significant (see Table S1 in the supplemental material). As the D124A substitution mutant induced a slightly higher level of apoptosis than the wild-type core protein (Fig. 6), a coimmunoprecipitation experiment also was performed to determine if this mutant can bind Mcl-1. Two different amounts of flag-tagged plasmids (0.5 and 1.0 μg) were used, and the results show that the D124A substitution mutant binds Mcl-1 to an extent similar to that of the wild-type core protein under both conditions (Fig. 7B).

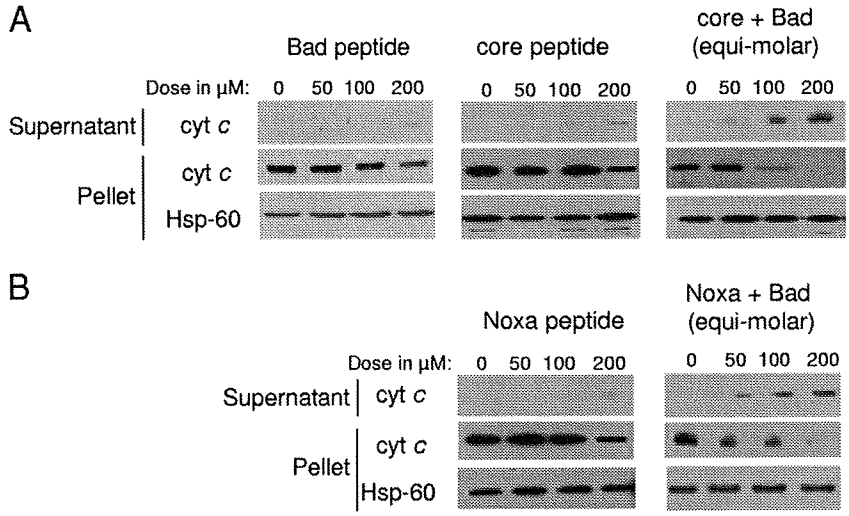

FIG. 5. Release of cytochrome *c* from isolated mitochondria by a combination of the core-BH3 and Bad-BH3 peptides or Noxa-BH3 and Bad-BH3 peptides. (A) Mitochondria isolated from 293T cells were incubated with either Bad peptide, core protein peptide, or a combination of the two peptides in equimolar concentrations. The total amount of peptide used in each experiment is indicated. Following centrifugation, the supernatants and pellets were subjected to Western blot analysis with anti-cytochrome *c* (cyt *c*) or anti-Hsp-60 antibodies. (B) The same experiment was repeated with Noxa peptide or a combination of Noxa and Bad peptides in equimolar concentrations.

While the V122 and L126 residues, at the h3 and h4 positions, respectively, of the core protein are highly conserved in different genotypes of HCV, the core proteins from genotype 2a strains typically have V instead of L at the h2 position (Fig. 1B). Replacing the L119 of the genotype 1b core protein with V reduced the proapoptotic property of the core protein dramatically (Fig. 8). Interestingly, in all known BH3-only proteins, this position is usually an L residue that is essential for the proapoptotic properties of these proteins (Fig. 1A). The reverse experiment was performed by determining if the core protein of a genotype 2a strain (JFH-1 strain) can induce apoptosis. The overexpression of the genotype 2a core protein induced much less apoptosis than the genotype 1b core protein (Fig. 8). However, replacing the V119 of the genotype 2a core protein with L resulted in a significant increase in apoptosis induction, such that the level was similar to that induced by the genotype 1b core protein (Fig. 8).

A single substitution from V to L at residue 119 in the core protein of the HCV J6/JFH-1 strain is associated with increased abilities to induce apoptosis. The pFL-J6/JFH-1 plasmid encoding the entire viral genome of a chimeric strain of HCV genotype 2a (J6/JFH-1) can be used to generate infectious HCV (37). In the J6/JFH-1 clone, the core protein contains V at residue 119, just like the JFH-1 clone. A mutant virus, J6/JFH-1(V119L), was generated successfully by replacing the V119 residue with L. Parental J6/JFH-1 and mutant J6/JFH-1(V119L) viruses then were used to infect naïve Huh7.5 cells, and cell viabilities were measured at different time points after infection (Fig. 9A). From day 2 p.i., cells infected by either virus have lower viabilities than mock-infected cells, indicating that the viruses have induced cytopathic effects (CPE). This is consistent with recent observations by us and other researchers (17, 41). Results from days 6 and 8 p.i. show that the J6/JFH-1(V119L) virus induced higher levels of CPE and, therefore, lower levels of cell viability compared to those of the parental J6/JFH-1 virus (Fig. 9A), which is in agreement with the overexpression studies shown in Fig. 8. The CPE is mediated primarily through apoptosis, as indicated by the activation of caspase-3 (Fig. 9B) and DNA fragmentation (Fig. 9C). The production of cell-free infectious virus particles by the J6/JFH-1(V119L) virus also was significantly higher than that produced by the parental J6/JFH-1 virus (Fig. 9D). On the other hand, there was no significant difference in the percentage of HCV-infected cells in the cultures (Fig. 9E) or HCV RNA replication in the cells between the two viruses (Fig. 9F). We next analyzed the possible interaction between endogenous Mcl-1 and the core proteins of either J6/JFH-1 or J6/JFH-1(V119L) in virus-infected cells. As shown in Fig. 9G, the core protein of J6/JFH-1(V119L) was coimmunoprecipitated with Mcl-1 (lane 6). On the other hand, the Mcl-1 interaction of the core protein of J6/JFH-1 was barely detected under the same experimental conditions (lane 4). These results collectively imply the possibility that the V119L mutation of the core protein promotes its interaction with Mcl-1 and is responsible for the increased ability of the virus to induce apoptosis, which favors a higher degree of infectious progeny virus release from the host cell at the late time points of infection compared to that of the parental J6/JFH-1 virus.

DISCUSSION

Besides playing important roles in maintaining homeostasis in healthy cells through the regulation of apoptosis, members of the Bcl-2 family also are involved in viral infections. Indeed, several viruses have been shown to encode homologs of prosurvival Bcl-2 proteins, and these viral proteins act to inhibit apoptosis in infected cells and prevent the premature death of these cells (see reviews in references 14, 26, 51, and 70). Other viral proteins, which can be proapoptotic, prosurvival, or both, do not share any sequence homology with members of the Bcl-2 family but also can modulate apoptosis in the host cells

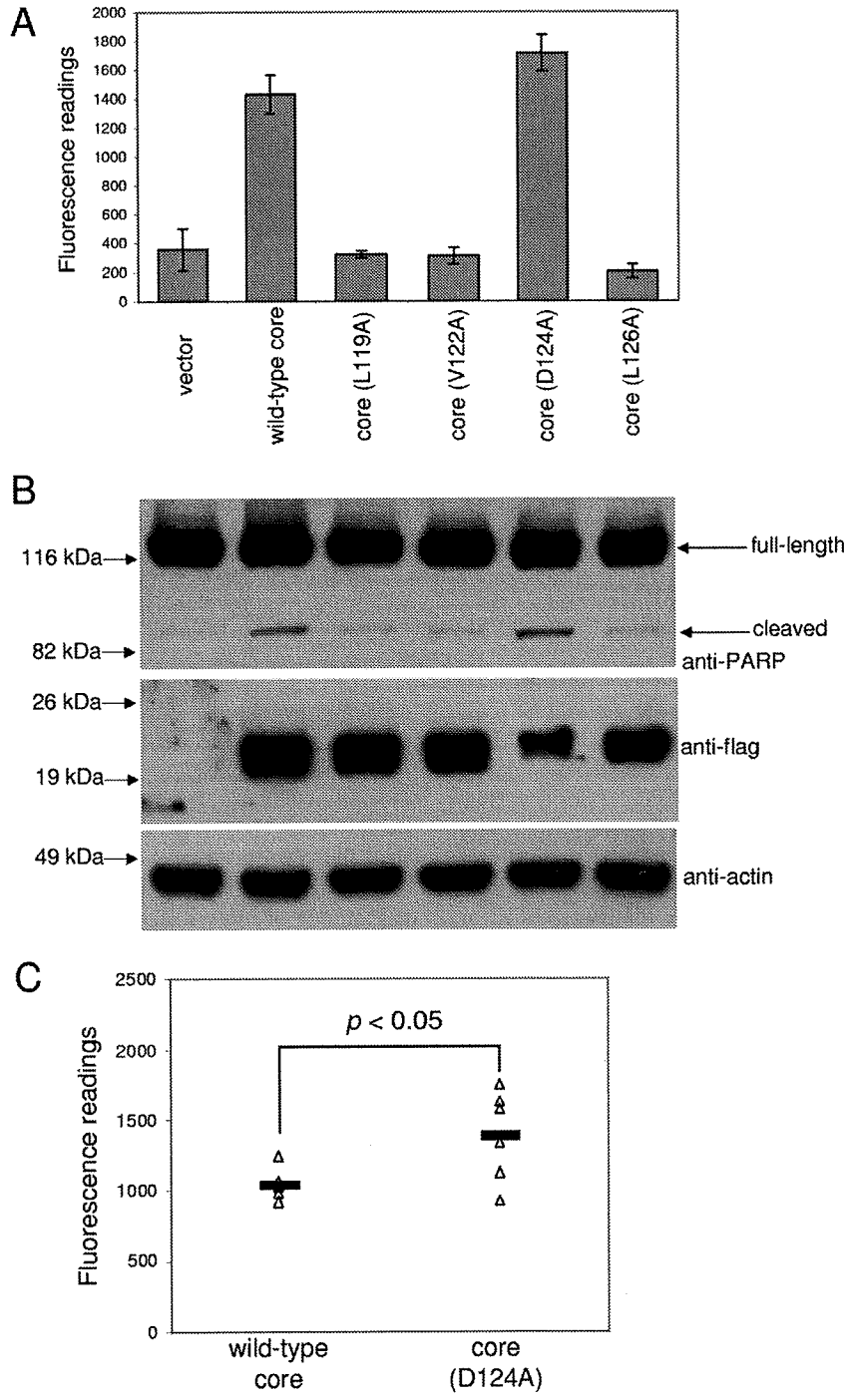

FIG. 6. Effects of alanine substitutions on the proapoptotic property of the core protein. (A) A CaspACE fluorometric assay system from Promega Corporation (Madison, WI) was used to measure the activation of caspase-3 in Huh7 cells that were transfected with vector only, wild-type core, or alanine substitution mutants. All experiments were performed in triplicate, and the average values with standard deviations are plotted. (B) Western blot analysis also was performed to determine the cleavage of endogenous PARP (top) and expression levels of the core proteins (middle). The amounts of total cell lysates loaded were verified by measuring the levels of endogenous actin (bottom). (C) The levels of activated caspase-3 induced by the wild-type core protein and the D124A mutant in six independent experiments were compared using the two-tailed Student's *t* test, and the difference was found to be statistically significant ($P < 0.05$). The values from each of the experiments are plotted as open triangles, and the average values are plotted as solid lines.

by interfering at different apoptotic checkpoints (see reviews in references 8, 23, 27, and 43).

Unlike the multi-BH domain members, the BH3-only members of the Bcl-2 family contain a single BH3 domain. Although all BH3-only proteins can bind to the hydrophobic grooves on the surfaces of the prosurvival members, recent quantitative measurements have revealed that the affinities of association between different pairs of BH3-only and prosur-

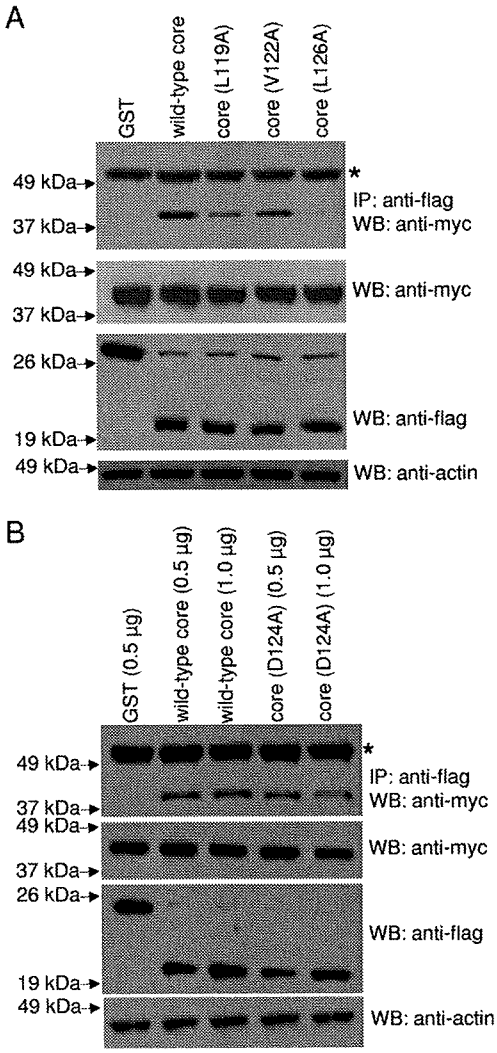

FIG. 7. Effects of alanine substitutions on the binding of the core protein to Mcl-1. (A) Huh7 cells were transfected with cDNA constructs (1.0 μg) for expressing flag-GST (negative control), flag-tagged wild-type core protein, or single-alanine-substitution mutants (L119A, V122A, and L126A). All cells were cotransfected with myc-tagged Mcl-1 (1.5 μg). (B) Huh7 cells were transfected with cDNA constructs for expressing flag-GST (negative control, 0.5 μg), flag-tagged wild-type core protein (0.5 or 1.0 μg), or single-alanine-substitution mutant D124A (0.5 or 1.0 μg). All cells were cotransfected with myc-tagged Mcl-1 (1.5 μg). Coimmunoprecipitation then was performed as described in the legend to Fig. 3A. The amount of myc-tagged proteins that coimmunoprecipitated (IP) with the flag-tagged proteins was determined by Western blot analysis (WB) with an anti-myc rabbit polyclonal antibody (top). The amounts of myc-tagged and flag-tagged proteins in the lysates before IP were determined by subjecting aliquots of the lysates to Western blot analysis (middle). The amounts of total cell lysates loaded were verified by measuring the levels of endogenous actin (bottom). The protein marked with an asterisk represents the heavy chain of the antibody used for IP (top). Similar results were obtained in four independent experiments, and a representative set of data is presented.

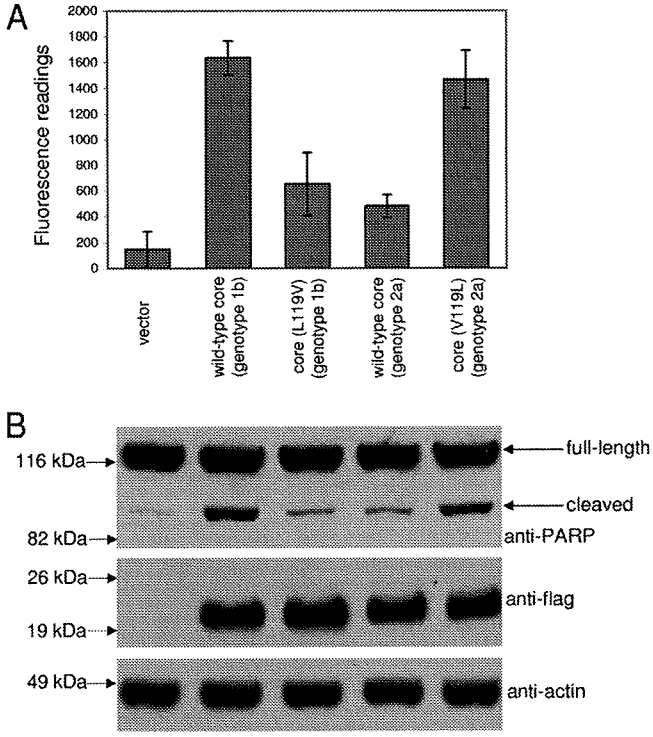

FIG. 8. Comparison of the proapoptotic properties of the core proteins of genotypes 1b and 2a. (A) A CaspACE fluorometric assay system from Promega Corporation (Madison, WI) was used to measure the activation of caspase-3 in Huh7 cells that were transfected with vector only, wild-type core of genotype 1b or 2a, or their substitution mutants. All experiments were performed in triplicate, and the average values with standard deviations are plotted. (B) Western blot analysis also was performed to determine the cleavage of endogenous PARP (top) and expression levels of the core proteins (middle). The amounts of total cell lysates loaded were verified by measuring the levels of endogenous actin (bottom).

vival members vary greatly (11, 32). For example, Bim and Puma bind all prosurvival members tested, while Noxa binds strongly only to Mcl-1 and A1. On the other hand, Bad binds much more strongly to Bcl-2, Bcl-X_L, and Bcl-w than Mcl-1. Taken together with results from successive studies, it becomes clear that the BH3-only members can be classified into subclasses (see reviews in references 21, 24, 58, and 71). In this study, we demonstrate that the HCV core protein is a BH3-only viral homologue of the Bcl-2 family, and its BH3 domain is essential for the induction of apoptosis (Fig. 1 and 2). In coimmunoprecipitation experiments, the core protein interacted specifically with the prosurvival Mcl-1 protein but not with prosurvival proteins Bcl-X_L and Bcl-w (Fig. 3), suggesting that its property is most similar to that of Noxa (11). Consistently, the overexpression of Mcl-1 protects against core protein-induced apoptosis (Fig. 4). However, the overexpression of Bcl-X_L also protects against core protein-induced apoptosis (Fig. 4). This may be due to the ability of a high level of Bcl-X_L to prevent the complementation between the core protein and endogenous Bad protein, which binds strongly to Bcl-X_L (11), as we have observed that a combination of the core protein and Bad peptide mimetics caused efficient cytochrome *c* release from the mitochondria (Fig. 5). The complementation between Bad and the core protein is similar to that observed between Bad and Noxa, which act in combination to neutralize the two classes of prosurvival proteins, one comprised of Bcl-2, Bcl-X_L, and Bcl-w and the other of Mcl-1 and A1 (11). In overexpres-

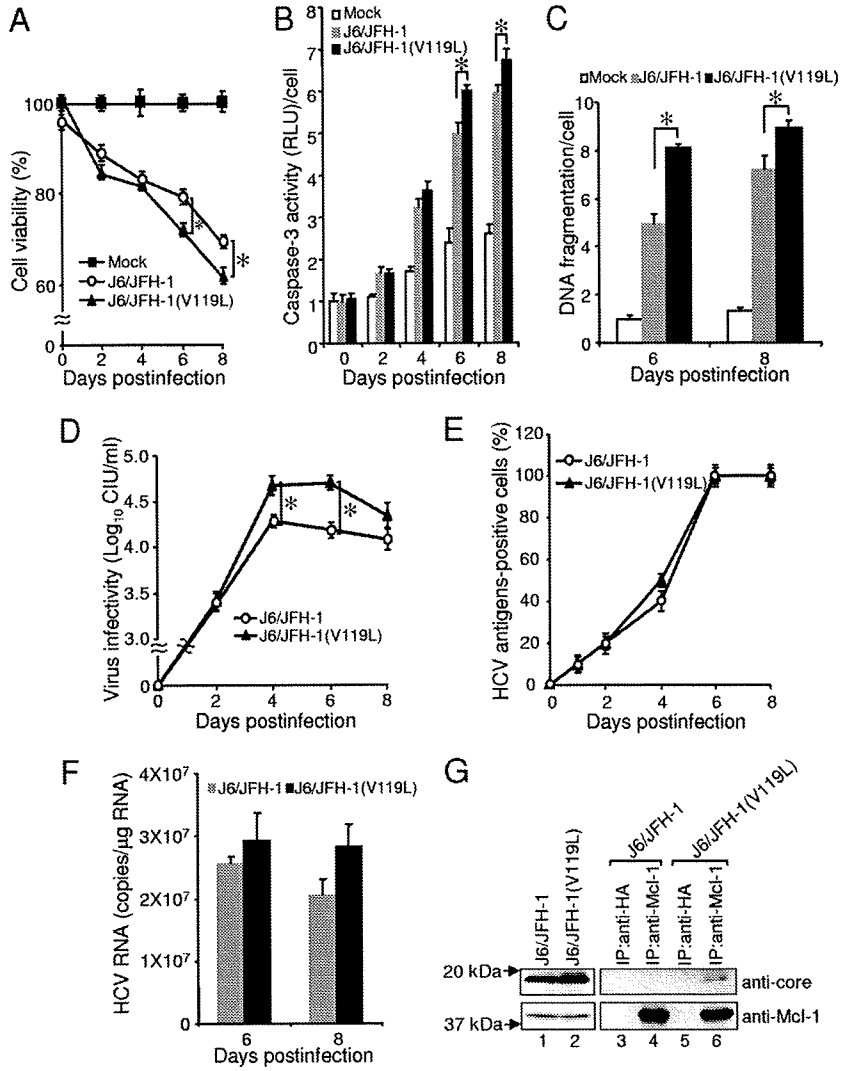

FIG. 9. Comparison of parental J6/JFH-1 and mutant J6/JFH-1(V119L) recombinant viruses. Huh7.5 cells were infected with recombinant HCV at a multiplicity of infection of 0.1 CIU/cell or with a mock preparation, and various assays were performed at different days after infection. (A) Cell viabilities were determined. (B) Caspase-3 activity per cell was determined. (C) The amount of DNA fragmentation per cell was determined. (D) The production of cell-free infectious virus particles was determined. (E) Virus spread in the culture was quantitated. (F) HCV RNA replication was determined by quantitative real-time PCR analysis. (G) Interaction of the core protein with Mcl-1 was determined by coimmunoprecipitation experiments at 3 days p.i. IP was performed using anti-Mcl-1 or anti-HA rabbit polyclonal antibodies and protein A agarose beads. The amounts of the core protein in the lysates before (lanes 1 and 2) and after IP (lanes 3 to 6) were determined by Western blot analysis with an anti-core monoclonal antibody (top). Similarly, the amounts of endogenous Mcl-1 in the samples were determined using an anti-Mcl-1 monoclonal antibody (bottom). Statistical analysis was performed using the one-way analysis of variance to determine if the differences between parental and mutant viruses were statistically significant, and those with P values of <0.05 (marked by asterisks) are considered statistically significant. Data were obtained from three independent experiments, each with triplicate cultures.

sion studies, the core protein and Noxa also induced comparable levels of apoptosis (see Fig. S3 and S5 in the supplemental material). Taken together, these findings suggest that core can mimic Noxa and interfere directly with the prosurvival function of Mcl-1.

A comparison of the BH3 domain of the core protein to the corresponding domains of other BH3-containing proteins (Fig. 1A) revealed that it contains three out of the four hydrophobic residues that can be accommodated within the hydrophobic pockets of previously described BH3 binding grooves (see reviews in references 50 and 69). Alanine substitution experiments revealed that all three hydrophobic residues in the BH3 domain of the core protein are essential for apoptosis induction (Fig. 6). In coimmunoprecipitation experiments, these alanine substitution mutants also bound Mcl-1 to a lesser extent than the wild-type core protein (Fig. 7A). Since these alanine substitution mutants still can bind Mcl-1, albeit at a lower level than that of the wild-type core protein, it appears that the interactions between these mutants and Mcl-1 are not sufficient to induce apoptosis. In several mutagenesis studies, the interaction between Bcl-2 family members and apoptosis regulation have been observed to be discordant. For example, two mutants of the BH3-only protein Bik, Bik-(43-94) and Bik-(43-120), heterodimerized with prosurvival Bcl-2 and Bcl-X_L but

were unable to induce efficient cell death (19). A Bad mutant containing an alteration of a critical residue within its BH3 domain, E113 to K, also was found to have significantly reduced apoptotic activity compared to that of wild-type Bad, despite binding to Bcl-2 and/or Bcl-X_L to the same extent as wild-type Bad (35). Therefore, the induction of apoptosis by the core protein may be controlled by a critical threshold affinity of binding between the core protein and Mcl-1, or there are contributions from a yet-to-be characterized pathway(s). Two of these residues (V122 and L126) are conserved in the major genotypes of HCV, but residue 119 is a V in genotype 2a (Fig. 1B). When L119 of the genotype 1b core protein was replaced with V, its ability to induce apoptosis was greatly reduced (Fig. 8). Conversely, when V119 of the genotype 2a core protein was replaced with L, its ability to induce apoptosis was greatly enhanced. Thus, the results suggest that the genotype 1b core protein induces apoptosis efficiently via a BH3 domain, while genotype 2a core protein is comparatively less efficient. Another highly conserved residue in the BH3 domain of the core protein is D124. However, the replacement of D124 with A did not reduce the proapoptotic function of the core protein (Fig. 6). Thus far, there are only a few known functional BH3 domains that do not contain D at this position (61, 62). Unlike most BH3-only proteins, the core protein has a charged residue (R115) in the h1 position (Fig. 1A). Interestingly, the second BH3 domain of mouse Noxa (mNoxaB) also has a charged residue (E74) in this position. Indeed, the nuclear magnetic resonance structure of the complex between mouse Mcl-1 and a peptide mimetic of mNoxaB shows that E74 is tolerated at the h1 position because its charged carboxyl group is coordinated by another charged residue, K215, in mouse Mcl-1 (15). However, R115 of the core protein is basic instead of acidic, and how this residue can be accommodated in the hydrophobic groove of Mcl-1 is unclear. Interestingly, replacing the residue at the h1 position (I58) of a novel BimBH3 variant, Bim_s2A, with A also has little effect on its interaction with Mcl-1 (34). Thus, it appears that the residue in the h1 position is not always involved in the interaction between BH3-only proteins and Mcl-1, but further biophysical and biochemical studies are required to delineate the precise structure-function relationship for the interaction between core and Mcl-1.

To determine if the results from overexpression studies are relevant to the modulation of apoptosis in host cells during HCV infection, the J6/JFH-1-based (genotype 2a) system was used to generate HCV carrying a substitution at residue 119 of the core protein. While the parental wild-type and mutant viruses replicated efficiently in Huh7.5 cells, the J6/JFH-1(V119L) virus (which expresses the core protein with L at the h2 position of the BH3 domain) caused a significantly higher level of apoptosis in the infected cells than the parental J6/JFH-1 virus (which expresses the core protein with V at the h2 position of the BH3 domain) (Fig. 9). This is in good agreement with the overexpression studies and indicates that the BH3 domain of the core protein contributes to the induction of apoptosis in HCV-infected cells. Thus, it appears that core protein-mediated apoptosis during infection by HCV of genotype 2a is less efficient than that of the other genotypes having L at residue 119 of the core protein (Fig. 1B). Coimmunoprecipitation experiments revealed that the core protein of J6/JFH-1(V119L), but not that of J6/JFH-1, interacted with Mcl-1 in virus-infected cells (Fig. 9). This result is consistent with the overexpression studies and suggests the possibility that the core protein induces apoptosis, at least partly, through the interaction with Mcl-1 in HCV-infected cells. Interestingly, more progeny virus is released from cells infected with the J6/JFH-1(V119L) virus than by those infected with the parental J6/JFH-1, while there is no difference in the efficiency of infection or amount of HCV replication inside the cells (Fig. 9).

However, it also is apparent that the parental J6/JFH-1 virus still caused a high level of apoptosis in the infected cells, and for the early time points there was no significant difference in the levels of apoptosis induced by the parental J6/JFH-1 virus and the J6/JFH-1(V119L) mutant virus (Fig. 9). This implies that there are other viral factors that contribute to the induction of apoptosis during HCV infection. For example, several nonstructural HCV proteins, like NS3, NS4A, NS5A, and NS5B, can induce apoptosis when they are overexpressed in certain types of cells (see recent reviews in references 20 and 28). In addition, other domains in the core protein have been shown to bind host proteins and may contribute to apoptosis regulation by interfering with different cellular pathways (see reviews in references 33, 42, and 52). For example, the N-terminal domain (aa 1 to 75) of the core protein interacts with Hsp60, leading to the production of reactive oxygen species and enhancement of tumor necrosis factor alpha-mediated apoptosis (30), while a C-terminal domain (aa 153 to 192) facilitates Fas oligomerization and is required for apoptosis induction in Jurkat cells (46). However, the relative contribution of these various factors to apoptosis induction during HCV infection remains to be determined.

We further examined the importance of residue 119 of the core protein in HCV replication. In multiple independent transfection experiments, we observed that the J6/JFH-1 mutant possessing A at position 119 [J6/JFH-1(V119A)] barely replicated in the cells and did not produce any infectious virus particles in the culture supernatants (data not shown). This result suggests the possibility that this single point mutation impairs the interaction of the core protein with other viral and/or cellular protein(s) that is required for HCV RNA replication and infectious virion production. Similarly, the J6/JFH-1 mutants each possessing A at positions 122 [J6/JFH-1(V122A)], 124 [J6/JFH-1(D124A)], or 126 [J6/JFH-1(L126A)] barely replicated in the cells and did not produce any infectious virion in the culture supernatants (data not shown), with the results suggesting an important role(s) for these residues as well as for position 119. In this connection, the essential role for the HCV core protein in infectious virion production recently has been confirmed, and numerous residues required for this role have been identified (47).

By using the JFH-1 infectious clone, recent studies have revealed that the association of the core protein with the lipid droplet (LD) is critical for the production of infectious virus particles (6, 45). Boulant and coworkers reported that there are two amphipathic α-helices in the so-called D2 domain of the core protein (~118 to 179 aa) (5, 7), and the hydrophobic residues within this domain are critical for the efficient attachment of the core protein to LD (5). Our results showed that residues L119, V122, and L126 of the core protein are essential

for the induction of apoptosis, and these residues are found on the hydrophobic face of the first α-helix of the D2 domain. Interestingly, the replacement of L119 with E did not affect LD association, while the replacement of L126 with E significantly reduced LD association (5). The contribution of V122 to LD association was not investigated. Consistently, the J6/JFH-1(V119L) virus, but not the J6/JFH-1(L126A) virus, replicated efficiently to produce infectious virus particles. Since L119 of the genotype 1b core protein, which occupies the crucial h2 position in the BH3 domain, is essential for its proapoptotic property but not for its association with LD, it is clear that the BH3 domain of the core protein is an independent motif that partially overlaps with the LD association domain.

Recently, Makes caterpillars floppy 1 (Mcf1), a bacterial toxin, was reported to contain a BH3-like domain (18). In addition, HBSP, a spliced hepatitis B viral protein, also contains a BH3-like domain (39). Here, we show that the HCV core protein is another BH3-like viral homologue, and it contributes directly to the induction of apoptosis during HCV infection. Our results also reveal that it is a bona fide BH3-only protein that appears to interfere with the prosurvival property of Mcl-1 in a manner similar to that of Noxa. Our observation that the enhanced apoptotic activity of the J6/JFH-1(V119L) virus is correlated with an increase in infectious progeny HCV release seems to be counterintuitive, as many viruses adopted strategies to prevent apoptosis in the infected cells so as to allow viral replication and the packaging of progeny genomes within the cells (14, 26, 51, 70). However, enhanced releases of virus from infected cells that are undergoing apoptosis also have been reported for other viruses, like the infectious bursal disease virus, adenovirus, and Aleutian mink disease parvovirus (4, 44, 73), indicating that apoptosis can be advantageous for viral spreading at the late stages of infection. Future studies to define the precise manner by which the BH3 domain of the core protein modulates apoptosis during infection will provide important insights into HCV replication as well as pathogenesis.

Besides the genotype 1b core protein, the properties of the genotype 1a core protein also have been examined in various studies. The apoptotic property of the genotype 1a core protein has yet to be studied using the JFH-1-based infectious clone system, although previous studies have attributed both prosurvival and proapoptotic properties to it (25, 30, 46, 57). Similar observations also have been described in overexpression studies using the genotype 1b core protein and appear to be dependent on the death stimuli and types of cells used (3, 9, 10, 36, 49, 53, 56, 60, 76). Several studies have identified domains or regions within the core protein that interfere with specific apoptosis pathways. For instance, the interaction of the N-terminal domain (residues 1 to 75) of the genotype 1a core protein with Hsp60 enhanced tumor necrosis factor alpha-mediated apoptosis, while its C-terminal region (residues 153 to 192) is required for Fas ligand-independent apoptosis (30, 46). The genotype 1b core protein (residues 1 to 153) binds to the death domain of FADD, resulting in enhanced apoptosis (76). However, an overlapping domain spanning the first 46 aa of the core protein is involved in ASPP2 interaction, which leads to the inhibition of p53-mediated apoptosis (9). These findings suggest that multiple domains present in the core protein contribute to the modulation of apoptosis via diverse pathways. Therefore, the net apoptotic effect of the core protein may be dependent on the relative strength of its prosurvival and proapoptotic properties. Unlike the genotype 2a core protein, the BH3 domains of the genotype 1b core protein and the genotype 1a core protein share an identical sequence (Fig. 1B) and are expected to function in a similar manner. However, we cannot rule out that there may be differences in the manner in which the core proteins of genotypes 1a and 1b modulate apoptosis during infection. For example, they may be involved in different virus-virus or virus-host interactions. Thus, more studies are needed to understand the contributions of genotype-dependent factors to the regulation of apoptosis during HCV infection.

ACKNOWLEDGMENTS

We thank T. Wakita for the JFH-1 construct and anti-core monoclonal antibody and C. M. Rice for the J6/JFH-1 construct and Huh7.5 cells.

This work was supported by the Biomedical Research Council of A*STAR (Agency for Science, Technology and Research), Singapore, a Health and Labor Sciences Research Grant from the Ministry of Health, Labor and Welfare, Japan, and the Program of Founding Research Centers for Emerging and Reemerging Infectious Diseases, the Ministry of Education, Culture, Sports, Science and Technology, Japan.

Y.-J.T. is an adjunct staff member of the Department of Microbiology at the National University of Singapore.

REFERENCES

1. **Adams, J. M., and S. Cory.** 2007. Bcl-2-regulated apoptosis: mechanism and therapeutic potential. Curr. Opin. Immunol. **19:**488–496.
2. **Bartenschlager, R., and V. Lohmann.** 2000. Replication of hepatitis C virus. J. Gen. Virol. **81:**1631–1648.
3. **Benali-Furet, N. L., M. Chami, L. Houel, F. De Giorgi, F. Vernejoul, D. Lagorce, L. Buscail, R. Bartenschlager, F. Ichas, R. Rizzuto, and P. Paterlini-Brechot.** 2005. Hepatitis C virus core triggers apoptosis in liver cells by inducing ER stress and ER calcium depletion. Oncogene **24:**4921–4933.
4. **Best, S. M., J. B. Wolfinbarger, and M. E. Bloom.** 2002. Caspase activation is required for permissive replication of Aleutian mink disease parvovirus in vitro. Virology **292:**224–234.
5. **Boulant, S., R. Montserret, R. G. Hope, M. Ratinier, P. Targett-Adams, J. P. Lavergne, F. Penin, and J. McLauchlan.** 2006. Structural determinants that target the hepatitis C virus core protein to lipid droplets. J. Biol. Chem. **281:**22236–22247.
6. **Boulant, S., P. Targett-Adams, and J. McLauchlan.** 2007. Disrupting the association of hepatitis C virus core protein with lipid droplets correlates with a loss in production of infectious virus. J. Gen. Virol. **88:**2204–2213.
7. **Boulant, S., C. Vanbelle, C. Ebel, F. Penin, and J. P. Lavergne.** 2005. Hepatitis C virus core protein is a dimeric alpha-helical protein exhibiting membrane protein features. J. Virol. **79:**11353–11365.
8. **Boya, P., A. L. Pauleau, D. Poncet, R. A. Gonzalez-Polo, N. Zamzami, and G. Kroemer.** 2004. Viral proteins targeting mitochondria: controlling cell death. Biochim. Biophys. Acta **1659:**178–189.
9. **Cao, Y., T. Hamada, T. Matsui, T. Date, and K. Iwabuchi.** 2004. Hepatitis C virus core protein interacts with p53-binding protein, 53BP2/Bbp/ASPP2, and inhibits p53-mediated apoptosis. Biochem. Biophys. Res. Commun. **315:**788–795.
10. **Chang, M. L., J. C. Chen, M. Y. Chang, C. T. Yeh, W. P. Lin, C. K. Liang, S. F. Huang, K. N. Dang, C. T. Chiu, and D. Y. Lin.** 2008. Acute expression of hepatitis C core protein in adult mouse liver: mitochondrial stress and apoptosis. Scand. J. Gastroenterol. **43:**747–755.
11. **Chen, L., S. N. Willis, A. Wei, B. J. Smith, J. I. Fletcher, M. G. Hinds, P. M. Colman, C. L. Day, J. M. Adams, and D. C. Huang.** 2005. Differential targeting of prosurvival Bcl-2 proteins by their BH3-only ligands allows complementary apoptotic function. Mol. Cell **17:**393–403.
12. **Cheng, E. H., D. G. Kirsch, R. J. Clem, R. Ravi, M. B. Kastan, A. Bedi, K. Ueno, and J. M. Hardwick.** 1997. Conversion of Bcl-2 to a Bax-like death effector by caspases. Science **278:**1966–1968.
13. **Chou, A. H., H. F. Tsai, Y. Y. Wu, C. Y. Hu, L. H. Hwang, P. I. Hsu, and P. N. Hsu.** 2005. Hepatitis C virus core protein modulates TRAIL-mediated apoptosis by enhancing Bid cleavage and activation of mitochondria apoptosis signaling pathway. J. Immunol. **174:**2160–2166.
14. **Cuconati, A., and E. White.** 2002. Viral homologs of BCL-2: role of apoptosis in the regulation of virus infection. Genes Dev. **16:**2465–2478.

15. **Czabotar, P. E., E. F. Lee, M. F. van Delft, C. L. Day, B. J. Smith, D. C. Huang, W. D. Fairlie, M. G. Hinds, and P. M. Colman.** 2007. Structural insights into the degradation of Mcl-1 induced by BH3 domains. Proc. Natl. Acad. Sci. USA **104**:6217–6222.
16. **Danial, N. N.** 2007. BCL-2 family proteins: critical checkpoints of apoptotic cell death. Clin. Cancer Res. **13**:7254–7263.
17. **Deng, L., T. Adachi, K. Kitayama, Y. Bungyoku, S. Kitazawa, S. Ishido, I. Shoji, and H. Hotta.** 2008. Hepatitis C virus infection induces apoptosis through a Bax-triggered, mitochondria-mediated, caspase-3-dependent pathway. J. Virol. **82**:10375–10385.
18. **Dowling, A. J., N. R. Waterfield, M. C. Hares, G. Le Goff, C. H. Streuli, and R. H. ffrench-Constant.** 2007. The Mcf1 toxin induces apoptosis via the mitochondrial pathway and apoptosis is attenuated by mutation of the BH3-like domain. Cell Microbiol. **9**:2470–2484.
19. **Elangovan, B., and G. Chinnadurai.** 1997. Functional dissection of the pro-apoptotic protein Bik. Heterodimerization with anti-apoptosis proteins is insufficient for induction of cell death. J. Biol. Chem. **272**:24494–24498.
20. **Fischer, R., T. Baumert, and H. E. Blum.** 2007. Hepatitis C virus infection and apoptosis. World J. Gastroenterol. **13**:4865–4872.
21. **Fletcher, J. I., and D. C. Huang.** 2008. Controlling the cell death mediators Bax and Bak: puzzles and conundrums. Cell Cycle **7**:39–44.
22. **Fu, N. Y., S. K. Sukumaran, and V. C. Yu.** 2007. Inhibition of ubiquitin-mediated degradation of MOAP-1 by apoptotic stimuli promotes Bax function in mitochondria. Proc. Natl. Acad. Sci. USA **104**:10051–10056.
23. **Galluzzi, L., C. Brenner, E. Morselli, Z. Touat, and G. Kroemer.** 2008. Viral control of mitochondrial apoptosis. PLoS Pathog. **4**:e1000018.
24. **Häcker, G., and A. Weber.** 2007. BH3-only proteins trigger cytochrome *c* release, but how? Arch. Biochem. Biophys. **462**:150–155.
25. **Hahn, C. S., Y. G. Cho, B. S. Kang, I. M. Lester, and Y. S. Hahn.** 2000. The HCV core protein acts as a positive regulator of fas-mediated apoptosis in a human lymphoblastoid T cell line. Virology **276**:127–137.
26. **Hardwick, J. M., and D. S. Bellows.** 2003. Viral versus cellular BCL-2 proteins. Cell Death Differ. **10**(Suppl. 1):S68–S76.
27. **Hay, S., and G. Kannourakis.** 2002. A time to kill: viral manipulation of the cell death program. J. Gen. Virol. **83**:1547–1564.
28. **Herzer, K., M. F. Sprinzl, and P. R. Galle.** 2007. Hepatitis viruses: live and let die. Liver Int. **27**:293–301.
29. **Hope, R. G., and J. McLauchlan.** 2000. Sequence motifs required for lipid droplet association and protein stability are unique to the hepatitis C virus core protein. J. Gen. Virol. **81**:1913–1925.
30. **Kang, S. M., S. J. Kim, J. H. Kim, W. Lee, G. W. Kim, K. H. Lee, K. Y. Choi, and J. W. Oh.** 2009. Interaction of hepatitis C virus core protein with Hsp60 triggers the production of reactive oxygen species and enhances TNF-alpha-mediated apoptosis. Cancer Lett. **279**:230–237.
31. **Kozopas, K. M., T. Yang, H. L. Buchan, P. Zhou, and R. W. Craig.** 1993. MCL1, a gene expressed in programmed myeloid cell differentiation, has sequence similarity to BCL2. Proc. Natl. Acad. Sci. USA **90**:3516–3520.
32. **Kuwana, T., L. Bouchier-Hayes, J. E. Chipuk, C. Bonzon, B. A. Sullivan, D. R. Green, and D. D. Newmeyer.** 2005. BH3 domains of BH3-only proteins differentially regulate Bax-mediated mitochondrial membrane permeabilization both directly and indirectly. Mol. Cell **17**:525–535.
33. **Lai, M. M., and C. F. Ware.** 2000. Hepatitis C virus core protein: possible roles in viral pathogenesis. Curr. Top. Microbiol. Immunol. **242**:117–134.
34. **Lee, E. F., P. E. Czabotar, M. F. van Delft, E. M. Michalak, M. J. Boyle, S. N. Willis, H. Puthalakath, P. Bouillet, P. M. Colman, D. C. Huang, and W. D. Fairlie.** 2008. A novel BH3 ligand that selectively targets Mcl-1 reveals that apoptosis can proceed without Mcl-1 degradation. J. Cell Biol. **180**:341–355.
35. **Lee, J. W., Y. H. Soung, S. Y. Kim, S. W. Nam, C. J. Kim, Y. G. Cho, J. H. Lee, H. S. Kim, W. S. Park, S. H. Kim, J. Y. Lee, N. J. Yoo, and S. H. Lee.** 2004. Inactivating mutations of proapoptotic Bad gene in human colon cancers. Carcinogenesis **25**:1371–1376.
36. **Lee, S. K., S. O. Park, C. O. Joe, and Y. S. Kim.** 2007. Interaction of HCV core protein with 14-3-3epsilon protein releases Bax to activate apoptosis. Biochem. Biophys. Res. Commun. **352**:756–762.
37. **Lindenbach, B. D., M. J. Evans, A. J. Syder, B. Wolk, T. L. Tellinghuisen, C. C. Liu, T. Maruyama, R. O. Hynes, D. R. Burton, J. A. McKeating, and C. M. Rice.** 2005. Complete replication of hepatitis C virus in cell culture. Science **309**:623–626.
38. **Liu, Q., C. Tackney, R. A. Bhat, A. M. Prince, and P. Zhang.** 1997. Regulated processing of hepatitis C virus core protein is linked to subcellular localization. J. Virol. **71**:657–662.
39. **Lu, Y. W., T. L. Tan, V. Chan, and W. N. Chen.** 2006. The HBSP gene is expressed during HBV replication, and its coded BH3-containing spliced viral protein induces apoptosis in HepG2 cells. Biochem. Biophys. Res. Commun. **351**:64–70.
40. **Marusawa, H., M. Hijikata, T. Chiba, and K. Shimotohno.** 1999. Hepatitis C virus core protein inhibits Fas- and tumor necrosis factor alpha-mediated apoptosis via NF-κB activation. J. Virol. **73**:4713–4720.
41. **Mateu, G., R. O. Donis, T. Wakita, J. Bukh, and A. Grakoui.** 2008. Intragenotypic JFH1 based recombinant hepatitis C virus produces high levels of infectious particles but causes increased cell death. Virology **376**:397–407.
42. **McLauchlan, J.** 2000. Properties of the hepatitis C virus core protein: a structural protein that modulates cellular processes. J. Viral Hepat. **7**:2–14.
43. **McLean, J. E., A. Ruck, A. Shirazian, F. Pooyaei-Mehr, and Z. F. Zakeri.** 2008. Viral manipulation of cell death. Curr. Pharm. Des. **14**:198–220.
44. **Mi, J., Z. Y. Li, S. Ni, D. Steinwaerder, and A. Lieber.** 2001. Induced apoptosis supports spread of adenovirus vectors in tumors. Hum. Gene Ther. **12**:1343–1352.
45. **Miyanari, Y., K. Atsuzawa, N. Usuda, K. Watashi, T. Hishiki, M. Zayas, R. Bartenschlager, T. Wakita, M. Hijikata, and K. Shimotohno.** 2007. The lipid droplet is an important organelle for hepatitis C virus production. Nat. Cell Biol. **9**:1089–1097.
46. **Moorman, J. P., D. Prayther, D. McVay, Y. S. Hahn, and C. S. Hahn.** 2003. The C-terminal region of hepatitis C core protein is required for Fas-ligand independent apoptosis in Jurkat cells by facilitating Fas oligomerization. Virology **312**:320–329.
47. **Murray, C. L., C. T. Jones, J. Tassello, and C. M. Rice.** 2007. Alanine scanning of the hepatitis C virus core protein reveals numerous residues essential for production of infectious virus. J. Virol. **81**:10220–10231.
48. **Nomura-Takigawa, Y., M. Nagano-Fujii, L. Deng, S. Kitazawa, S. Ishido, K. Sada, and H. Hotta.** 2006. Non-structural protein 4A of hepatitis C virus accumulates on mitochondria and renders the cells prone to undergoing mitochondria-mediated apoptosis. J. Gen. Virol. **87**:1935–1945.
49. **Otsuka, M., N. Kato, H. Taniguchi, H. Yoshida, T. Goto, Y. Shiratori, and M. Omata.** 2002. Hepatitis C virus core protein inhibits apoptosis via enhanced Bcl-xL expression. Virology **296**:84–93.
50. **Petros, A. M., E. T. Olejniczak, and S. W. Fesik.** 2004. Structural biology of the Bcl-2 family of proteins. Biochim. Biophys. Acta **1644**:83–94.
51. **Polster, B. M., J. Pevsner, and J. M. Hardwick.** 2004. Viral Bcl-2 homologs and their role in virus replication and associated diseases. Biochim. Biophys. Acta **1644**:211–227.
52. **Ray, R. B., and R. Ray.** 2001. Hepatitis C virus core protein: intriguing properties and functional relevance. FEMS Microbiol. Lett. **202**:149–156.
53. **Realdon, S., M. Gerotto, F. Dal Pero, O. Marin, A. Granato, G. Basso, M. Muraca, and A. Alberti.** 2004. Proapoptotic effect of hepatitis C virus CORE protein in transiently transfected cells is enhanced by nuclear localization and is dependent on PKR activation. J. Hepatol. **40**:77–85.
54. **Ruggieri, A., T. Harada, Y. Matsuura, and T. Miyamura.** 1997. Sensitization to Fas-mediated apoptosis by hepatitis C virus core protein. Virology **229**: 68–76.
55. **Sabile, A., G. Perlemuter, F. Bono, K. Kohara, F. Demaugre, M. Kohara, Y. Matsuura, T. Miyamura, C. Brechot, and G. Barba.** 1999. Hepatitis C virus core protein binds to apolipoprotein AII and its secretion is modulated by fibrates. Hepatology **30**:1064–1076.
56. **Sacco, R., T. Tsutsumi, R. Suzuki, M. Otsuka, H. Aizaki, S. Sakamoto, M. Matsuda, N. Seki, Y. Matsuura, T. Miyamura, and T. Suzuki.** 2003. Anti-apoptotic regulation by hepatitis C virus core protein through up-regulation of inhibitor of caspase-activated DNase. Virology **317**:24–35.
57. **Saito, K., K. Meyer, R. Warner, A. Basu, R. B. Ray, and R. Ray.** 2006. Hepatitis C virus core protein inhibits tumor necrosis factor alpha-mediated apoptosis by a protective effect involving cellular FLICE inhibitory protein. J. Virol. **80**:4372–4379.
58. **Shibue, T., and T. Taniguchi.** 2006. BH3-only proteins: integrated control point of apoptosis. Int. J. Cancer. **119**:2036–2043.
59. **Soo, H. M., A. Garzino-Demo, W. Hong, Y. H. Tan, Y. J. Tan, P. Y. Goh, S. G. Lim, and S. P. Lim.** 2002. Expression of a full-length hepatitis C virus cDNA up-regulates the expression of CC chemokines MCP-1 and RANTES. Virology **303**:253–277.
60. **Takamatsu, M., T. Fujita, and H. Hotta.** 2001. Suppression of serum starvation-induced apoptosis by hepatitis C virus core protein. Kobe J. Med. Sci. **47**:97–112.
61. **Tan, K. O., K. M. Tan, S. L. Chan, K. S. Yee, M. Bevort, K. C. Ang, and V. C. Yu.** 2001. MAP-1, a novel proapoptotic protein containing a BH3-like motif that associates with Bax through its Bcl-2 homology domains. J. Biol. Chem. **276**:2802–2807.
62. **Tan, K. O., K. M. Tan, and V. C. Yu.** 1999. A novel BH3-like domain in BID is required for intramolecular interaction and autoinhibition of pro-apoptotic activity. J. Biol. Chem. **274**:23687–23690.
63. **Tan, Y. J., B. C. Fielding, P. Y. Goh, S. Shen, T. H. Tan, S. G. Lim, and W. Hong.** 2004. Overexpression of 7a, a protein specifically encoded by the severe acute respiratory syndrome coronavirus, induces apoptosis via a caspase-dependent pathway. J. Virol. **78**:14043–14047.
64. **Tan, Y. J., E. Teng, S. Shen, T. H. Tan, P. Y. Goh, B. C. Fielding, E. E. Ooi, H. C. Tan, S. G. Lim, and W. Hong.** 2004. A novel severe acute respiratory syndrome coronavirus protein, U274, is transported to the cell surface and undergoes endocytosis. J. Virol. **78**:6723–6734.
65. **Targett-Adams, P., G. Hope, S. Boulant, and J. McLauchlan.** 2008. Maturation of hepatitis C virus core protein by signal peptide peptidase is required for virus production. J. Biol. Chem. **283**:16850–16859.
66. **Uhlmann, E. J., T. Subramanian, C. A. Vater, R. Lutz, and G. Chinnadurai.** 1998. A potent cell death activity associated with transient high level expression of BCL-2. J. Biol. Chem. **273**:17926–17932.

67. **van Delft, M. F., and D. C. Huang.** 2006. How the Bcl-2 family of proteins interact to regulate apoptosis. Cell Res. **16**:203–213.
68. **Wakita, T., T. Pietschmann, T. Kato, T. Date, M. Miyamoto, Z. Zhao, K. Murthy, A. Habermann, H. G. Krausslich, M. Mizokami, R. Bartenschlager, and T. J. Liang.** 2005. Production of infectious hepatitis C virus in tissue culture from a cloned viral genome. Nat. Med. **11**:791–796.
69. **Walensky, L. D.** 2006. BCL-2 in the crosshairs: tipping the balance of life and death. Cell Death Differ. **13**:1339–1350.
70. **White, E.** 2006. Mechanisms of apoptosis regulation by viral oncogenes in infection and tumorigenesis. Cell Death Differ. **13**:1371–1377.
71. **Willis, S. N., and J. M. Adams.** 2005. Life in the balance: how BH3-only proteins induce apoptosis. Curr. Opin. Cell Biol. **17**:617–625.
72. **Yamanaka, T., M. Uchida, and T. Doi.** 2002. Innate form of HCV core protein plays an important role in the localization and the function of HCV core protein. Biochem. Biophys. Res. Commun. **294**:521–527.
73. **Yao, K., and V. N. Vakharia.** 2001. Induction of apoptosis in vitro by the 17-kDa nonstructural protein of infectious bursal disease virus: possible role in viral pathogenesis. Virology **285**:50–58.
74. **Yasui, K., T. Wakita, K. Tsukiyama-Kohara, S. I. Funahashi, M. Ichikawa, T. Kajita, D. Moradpour, J. R. Wands, and M. Kohara.** 1998. The native form and maturation process of hepatitis C virus core protein. J. Virol. **72**:6048–6055.
75. **Youle, R. J., and A. Strasser.** 2008. The BCL-2 protein family: opposing activities that mediate cell death. Nat. Rev. Mol. Cell Biol. **9**:47–59.
76. **Zhu, N., C. F. Ware, and M. M. Lai.** 2001. Hepatitis C virus core protein enhances FADD-mediated apoptosis and suppresses TRADD signaling of tumor necrosis factor receptor. Virology **283**:178–187.

Journal of General Virology (2009), 90, 1681–1691 DOI 10.1099/vir.0.010983-0

Efficient production of infectious hepatitis C virus with adaptive mutations in cultured hepatoma cells

Yasuaki Bungyoku, Ikuo Shoji, Tatsuhiko Makine, Tetsuya Adachi, Kazumi Hayashida, Motoko Nagano-Fujii, Yoshi-Hiro Ide, Lin Deng and Hak Hotta

Correspondence
Hak Hotta
hotta@med.kobe-u.ac.jp

Division of Microbiology, Kobe University Graduate School of Medicine, 7-5-1 Kusunoki-cho, Chuo-ku, Kobe, Hyogo 650-0017, Japan

Robust production of infectious hepatitis C virus (HCV) in cell culture was realized by using the JFH1 strain and the homologous chimeric J6/JFH1 strain in Huh-7.5 cells, a highly HCV-permissive subclone of Huh-7 cells. In this study, we aimed to establish a more efficient HCV-production system and to gain some insight into the adaptation mechanisms of efficient HCV production. By serial passaging of J6/JFH1-infected Huh-7.5 cells, we obtained culture-adapted J6/JFH1 variants, designated P-27, P-38 and P-47. Sequence analyses revealed that the adaptive mutant viruses P-27, P-38 and P-47 possessed eight mutations [four in E2, two in NS2, one in NS5A and one in NS5B), 10 mutations [two additional mutations in the 5′-untranslated region (5′-UTR) and core] and 11 mutations (three additional mutations in 5′-UTR, core and NS5B), respectively. We introduced amino acid substitutions into the wild-type J6/JFH1 clone, generated recombinant viruses with adaptive mutations and analysed their infectivity and ability to produce infectious viruses. The viruses with the adaptive mutations exhibited higher expression of HCV proteins than did the wild type in Huh-7.5 cells. Moreover, we provide evidence suggesting that the mutation N534H in the E2 glycoprotein of the mutant viruses conferred an advantage at the entry level. We thus demonstrate that an efficient HCV-production system could be obtained by introducing adaptive mutations into the J6/JFH1 genome. The J6/JFH1-derived mutant viruses presented here would be a good tool for producing HCV particles with enhanced infectivity and for studying the molecular mechanism of HCV entry.

Received 11 February 2009
Accepted 5 March 2009

INTRODUCTION

Hepatitis C virus (HCV) is the main cause of chronic hepatitis, liver cirrhosis and hepatocellular carcinoma (Choo *et al.*, 1989; Kuo *et al.*, 1989; Saito *et al.*, 1990). As more than 170 million people worldwide are infected chronically with HCV (Poynard *et al.*, 2003) and because the current antiviral therapy, interferon and ribavirin, produces sustained virus clearance in <50 % of treated patients (Manns *et al.*, 2007), HCV infection is clearly a problem of major proportions. HCV is a single-stranded, positive-sense RNA virus that is classified in the genus *Hepacivirus* in the family *Flaviviridae*. The approximately 9.6 kb HCV genome encodes one large open reading frame (ORF) that is flanked at the 5′ and 3′ ends by untranslated regions (UTRs) (Choo *et al.*, 1991). The HCV polyprotein is processed into at least 10 proteins by viral proteases and cellular signalases (Grakoui *et al.*, 1993; Hijikata *et al.*, 1993a; McLauchlan *et al.*, 2002). The structural proteins core, E1 and E2 are located in the N terminus of the polyprotein, followed by p7 and the non-structural (NS) proteins NS2, NS3, NS4A, NS4B, NS5A and NS5B (Bartenschlager & Sparacio, 2007).

Study of the HCV life cycle and virus–host interaction has been hampered severely by the lack of a robust *in vitro* cell-culture system and small-animal models of HCV infection (Bartenschlager & Sparacio, 2007). The development of HCV replicon systems has made an important contribution to the study of HCV translation and RNA replication in the human hepatoma cell line Huh-7 (Blight *et al.*, 2000; Lohmann *et al.*, 1999). Sequence analyses of multiple HCV replicons have revealed that several adaptive mutations enhance RNA replication to varying degrees (Bartenschlager & Sparacio, 2007; Blight *et al.*, 2000; Lohmann *et al.*, 2001). Such adaptive mutations were primarily identified in a central portion of the NS5A protein. Although the extent to which these adaptive mutations enhance RNA replication was subsequently studied by using various transient replication assays, the molecular mechanism underlying replication enhancement still remains elusive (Bartenschlager & Sparacio, 2007). The HCV replicons containing adaptive mutations do not produce infectious virus particles in culture and are severely attenuated (Blight *et al.*, 2002; Pietschmann *et al.*, 2002). Using recombinant HCV envelope glycoproteins

and HCV pseudoparticles, several cell-surface molecules have been shown to interact with HCV during virus binding and entry, including the tetraspanin CD81 (Bartosch *et al.*, 2003; Pileri *et al.*, 1998), the scavenger receptor class B member I (SR-BI) (Bartosch *et al.*, 2003; Scarselli *et al.*, 2002) and the tight junction protein claudin-1 (CLDN1) (Evans *et al.*, 2007).

The major breakthrough was made by establishing an HCV-production system using HCV strain JFH1, a genotype 2a isolate, and Huh-7 cells (Wakita *et al.*, 2005). Two other groups reported a robust production of infectious virus using a homologous chimeric FL-J6/JFH1 strain (Lindenbach *et al.*, 2005) or using Huh-7.5.1 cells (Zhong *et al.*, 2005) derived from the cell line Huh-7.5, which has a defect in the RIG-I pathway (Sumpter *et al.*, 2005). Upon transfection of Huh-7 cells with the *in vitro*-transcribed HCV JFH1 genome or the chimera FL-J6/JFH1, infectious HCV particles were secreted in an envelope glycoprotein-dependent manner (Lindenbach *et al.*, 2005; Wakita *et al.*, 2005; Zhong *et al.*, 2005). Using HCV-production systems, adaptive or compensatory mutations that promote the production of infectious virus from wild-type JFH1 (Delgrange *et al.*, 2007; Kaul *et al.*, 2007; Russell *et al.*, 2008; Zhong *et al.*, 2006) or chimeric viruses (Gottwein *et al.*, 2007; Yi *et al.*, 2006, 2007) have been identified. However, the molecular mechanisms of adaptive mutations are poorly understood.

In this study, we aimed to establish an efficient HCV-production system and to gain more insight into the determinants of efficient virus production. By serial passaging of Huh-7.5 cells infected with the HCV J6/JFH1 strain, we identified adaptive mutations in the clones and analysed the mutations by examining the production of the recombinant mutant viruses.

METHODS

Cell culture. Huh-7.5 cells (Blight *et al.*, 2002), a highly HCV-permissive subclone of Huh-7 cells, were kindly provided by Dr C. M. Rice (Rockefeller University, New York, NY, USA). Cells were cultured in Dulbecco's modified Eagle's medium (DMEM; Wako) supplemented with 10 % fetal bovine serum (FBS; Biowest), 0.1 mM non-essential amino acids (Invitrogen), 100 IU penicillin ml^{-1} and 100 μg streptomycin ml^{-1} (Invitrogen). DMEM containing 10 % FBS was designated complete DMEM. Cells were grown at 37 °C in a CO_2 incubator.

Antibodies. The mouse monoclonal antibodies (mAbs) used in this study were anti-core (2H9) mAb (Wakita *et al.*, 2005) and anti-HCV NS3 mAb (Chemicon). Goat anti-actin polyclonal antibody (C-11) (Santa Cruz Biotech) was used. Horseradish peroxidase (HRP)-conjugated goat anti-mouse IgG (MBL) and HRP-conjugated donkey anti-goat IgG (Santa Cruz Biotech) were used as secondary antibodies.

Plasmids. Plasmid pFL-J6/JFH1 (Lindenbach *et al.*, 2005) containing the full-length chimeric HCV genome was used to generate infectious HCV. Amino acid substitutions were introduced by site-directed mutagenesis using a QuikChange site-directed mutagenesis kit (Stratagene). All PCR-amplified DNA fragments were verified extensively by using an ABI PRISM 3100-Avant Genetic Analyzer (Applied Biosystems). The primer sequences used in this study are available from the authors upon request.

HCV RNA transfection and virus production. The pFL-J6/JFH1 plasmid was linearized with *Xba*I and *in vitro*-transcribed by using the T7 RiboMAX Express large-scale RNA production system (Promega) following the manufacturer's instructions. The quality of synthesized RNA was examined by agarose gel electrophoresis. Cells were trypsinized and washed with serum-free DMEM. In total, 6×10^6 cells were suspended in 500 μl serum-free DMEM and mixed with 10 μg *in vitro*-transcribed RNA in a 4 mm cuvette (Bio-Rad). The synthesized RNA was introduced into Huh-7.5 cells by electroporation using a Bio-Rad Gene Pulser system with a single pulse at 270 V, 975 μF. The cells were then plated in 10 cm culture dishes containing complete DMEM.

Indirect immunofluorescence. Immunofluorescence staining was performed essentially as described previously (Takigawa *et al.*, 2004). Cells seeded on glass coverslips in a 24-well plate at a density of 4×10^4 cells per well were infected with HCV. Cells were cultured, washed with PBS and fixed with 3.7 % paraformaldehyde in PBS for 10 min at room temperature, followed by permeabilization in 0.1 % Triton X-100 in PBS for 10 min at room temperature. After being washed twice with PBS, cells were blocked with 5 % goat serum in PBS and then incubated with the serum of an HCV-infected patient with a high titre of anti-HCV antibodies. Fluorescein isothiocyanate-conjugated goat anti-human IgG (MBL) was used as a secondary antibody. The cells were washed with PBS, counterstained with Hoechst 33342 solution (Molecular Probes) at room temperature for 10 min, mounted on glass slides and examined under a fluorescence microscope (BX51; Olympus).

Virus titration. Culture supernatants were diluted serially 10-fold in complete DMEM and used to infect 2×10^5 naïve Huh-7.5 cells per well in 24-well plates. The inoculum was incubated with cells for 6 h at 37 °C and then supplemented with fresh complete DMEM. The level of HCV infection was determined 1 day post-infection by immunofluorescence using anti-HCV polyclonal antibody. The virus titre was expressed in focus-forming units (ml supernatant)$^{-1}$ (f.f.u. ml^{-1}), as determined by the mean number of HCV-positive foci detected at the highest dilutions according to a previously described method (Zhong *et al.*, 2005).

Immunoblotting. Immunoblotting was performed essentially as described previously (Muramatsu *et al.*, 1997). To detect the expression of HCV proteins, the immune complexes were visualized by an ECL Western blotting detection kit (GE Healthcare) following the manufacturer's instructions.

HCV RNA quantification. Total RNA was extracted by using RNAiso (TaKaRa) according to the manufacturer's instructions. One microgram of isolated RNA was reverse-transcribed by using a QuantiTect reverse transcription kit (Qiagen) with random primers. RT-qPCR analysis was performed as described previously (Zhong *et al.*, 2005). HCV RNA was monitored by using the PCR primers 5′-TCTGCGGAACCGGTGAGTA-3′ (sense) and 5′-TCAGGCAGTA-CCACAAGGC-3′ (antisense). HCV transcript levels were determined relative to a standard curve comprising serial dilutions of plasmid containing the HCV J6/JFH1 cDNA.

HCV RNA genome sequencing. HCV RNA was isolated from 140 μl viral supernatant by using a QIAamp Viral RNA Mini kit (Qiagen), and then used as a template to generate cDNA in a reverse-transcription reaction using SuperScript One-Step RT-PCR with Platinum *Taq* (Invitrogen) according to the manufacturer's instruc-

tions. PCR primers of between 20 and 26 bases, designed using the sequence of J6/JFH1, were used to amplify four fragments of HCV cDNA (nt 49–3517, 2582–5966, 5832–8038 and 7870–9286) to cover most of the HCV genome. In addition, the 5′-end sequence was amplified by using the 5′ RACE System for Rapid Amplification of cDNA Ends (Invitrogen) and the 3′-end sequence was amplified by using a 3′-Full RACE Core set (TaKaRa). The sequences of the amplified DNA were determined by using an ABI PRISM 3100-Avant Genetic Analyzer.

Quantification of HCV core protein. HCV core protein in the cells or cell-culture supernatants was quantified by using a highly sensitive enzyme immunoassay (Ortho HCV antigen ELISA kit; Ortho Clinical Diagnostics). To determine intracellular amounts of core, cell lysates were prepared as described by Schaller *et al.* (2007).

Blocking of virus attachment and entry with anti-CD81 antibody. Blocking of virus attachment and entry with anti-CD81 antibody was performed essentially as described previously (Wakita *et al.*, 2005). Huh-7.5 cells (6×10^4 cells per 24-well plate) were pretreated with anti-CD81 antibody (clone JS-81; BD Biosciences) or an isotype-matched control antibody (purified mouse IgG1, κ isotype control; BD Biosciences) as indicated for 1 h. Cells were then infected with the wild-type or mutant viruses at an m.o.i. of 0.5 or 0.01 for 6 h. The viruses were removed, and the cells were washed with PBS and then supplemented with complete DMEM. The efficiency of infection was monitored 1 day after infection by counting the number of HCV-positive foci by immunofluorescence.

Statistical analysis. A two-tailed Student's *t*-test was applied to evaluate the statistical significance of differences measured from the datasets. A *P* value of <0.05 was considered to be statistically significant.

RESULTS

Increase in HCV infectivity titres during serial passage

To produce infectious HCV particles, *in vitro*-transcribed genomic J6/JFH1 RNA was electroporated into Huh-7.5 cells. Transfected Huh-7.5 cells were maintained and the infectivity titre of the culture supernatant reached 6×10^4 f.f.u. ml^{-1} at 20 days post-infection. This culture supernatant was designated P-1.

To generate higher infectivity titres for HCV, naïve Huh-7.5 cells (3×10^5 cells per six-well plate) were infected with 1 ml virus stock of P-1 (6×10^4 f.f.u. ml^{-1}) at an m.o.i. of 0.2 and the infected cells were passaged serially every 3–4 days to maintain a subconfluent culture for 6 months. The culture medium was replaced with fresh complete DMEM every day. The extracellular infectivity titres fluctuated in the beginning after transfection and became lowest at the 22nd passage (Fig. 1a). Thereafter, the extracellular infectivity titres increased again and reached highest infectivity at the 47th passage. Therefore, we further examined the supernatants at the 27th, 38th and 47th passages, and the viruses were designated P-27, P-38 and P-47, respectively. The infectivity titres were determined to be 7.0×10^3 f.f.u. ml^{-1} for P-27, 1.7×10^4 f.f.u. ml^{-1} for P-38 and 3.3×10^4 f.f.u. ml^{-1} for P-47 (Fig. 1a). These viruses were used as inocula in the following experiments.

Kinetics of virus production after infection with putative adaptive J6/JFH1 mutants

To examine the virus-production kinetics of these viruses in Huh-7.5 cells, naïve Huh-7.5 cells (3×10^4 cells per 24-well plate) were infected with each inoculum (6×10^3 f.f.u.) at an m.o.i. of 0.2. After infection, the culture supernatants were harvested each day for 10 days and assayed for infectivity titres (Fig. 1b). The P-1 virus showed a peak infectivity titre of 2.3×10^4 f.f.u. ml^{-1} at 4 days post-infection, whereas the P-27, P-38 and P-47 viruses showed peak titres of 1.0×10^6, 2.3×10^6 and 6.0×10^6 f.f.u. ml^{-1} at 4–5 days post-infection, respectively (Fig. 1b), suggesting that these three viruses produce infectious HCV particles more efficiently than the P-1 virus. The increased infectivity titres may have been due to an increase in the absolute number of released HCV particles or an increased proportion of infectious relative to non-infectious particles. To address this question, we compared the specific infectivities of the mutant viruses with those of the wild-type virus. The ratio of viral infectivity titre (f.f.u. ml^{-1}) to HCV RNA content [genome equivalents (GE) ml^{-1}] was determined as shown in Table 1. The mutant viruses, P-27, P-38 and P-47, had higher specific-infectivity titres (1 : 21, 1 : 10 and 1 : 10, respectively) than the wild-type virus P-1 (1 : 133), suggesting that the mutant viruses are more infectious than the wild type and that the mutant viruses possess adaptive mutations in the virus genomes.

Sequence analysis of genetic mutations in the adaptive mutants

To identify the genetic changes in the virus genomes that are responsible for the adaptation to Huh-7.5 cells, we sequenced the whole genomes of the viruses. No mutation was found in the P-1 virus, whereas several mutations were identified in the P-27, P-38 and P-47 viruses (Fig. 1c). The sequencing analysis of P-27 identified eight mutations that were located in the E2, NS2, NS5A and NS5B regions as follows: T396A, T416A, N534H and A712V in E2; Y852H and W879R in NS2; F2281L in NS5A; and M2876L in NS5B (Fig. 1c). P-38 possessed 10 mutations, the same mutations as in P-27 and two additional mutations. The additional mutations were found at nucleotide position 146 (U to A) in the 5′-UTR and an amino acid change, K78E, in the core region. P-47 contained 11 mutations, including the same 10 mutations as P-38 and one additional mutation, T2925A in NS5B. Thus, the first eight mutations were all present in the genomes of the three viruses, and the results suggested that these eight mutations contribute to the enhanced infectivity.

Effects of individual mutations on the production of infectious HCV

To determine which mutation is responsible for the enhancement of infectivity, recombinant genomes containing only one of the selected mutations were constructed

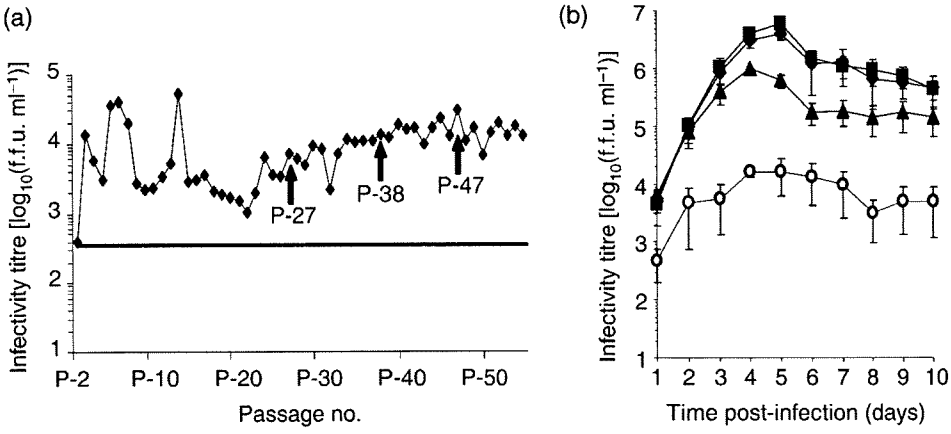

(c)

Virus	Position changed										
	5′-UTR	Core	E2				NS2		NS5A	NS5B	
	(nt 146)	78	396	416	534	712	852	879	2281	2876	2925
Wild-type	U	Lys	Thr	Thr	Asn	Ala	Tyr	Trp	Phe	Met	Thr
P-1	–	–	–	–	–	–	–	–	–	–	–
P-27	–	–	Ala	Ala	His	Val	His	Arg	Leu	Leu	–
P-38	A	Glu	Ala	Ala	His	Val	His	Arg	Leu	Leu	–
P-47	A	Glu	Ala	Ala	His	Val	His	Arg	Leu	Leu	Ala

Fig. 1. Increase in HCV infectivity titres during serial passage. (a) Serial passage of HCV J6/JFH1-infected Huh-7.5 cells. Huh-7.5 cells (3×10^5 cells per six-well plate) were infected with 1 ml stock of wild-type J6/JFH1 virus (P-1) (6×10^4 f.f.u. ml^{-1}) at an m.o.i. of 0.2, and the infected cells were passaged serially every 3–4 days to maintain a subconfluent culture for 6 months. The culture medium was replaced with fresh complete DMEM each day. The extracellular infectivity titres were determined by titration assay and are expressed as f.f.u. ml^{-1}. Arrows show the time points at which we collected the putative adapted viruses, designated P-27, P-38 and P-47. (b) Kinetics of virus production after infection with putative J6/JFH1 adaptive mutants in Huh-7.5 cells. Huh-7.5 cells were infected with the wild-type J6/JFH1 virus (○, P-1) or putative adaptive mutants (▲, P-27; ◆, P-38; ■, P-47) at an m.o.i. of 0.2. After infection, the culture supernatants were harvested every day until 10 days post-infection. Infectivity titres were measured by immunofluorescence assay and are expressed as f.f.u. ml^{-1}. Error bars represent SD for triplicate measurements. (c) Genetic mutations identified during passage. Numbers indicate the amino acid position where mutations were identified. The nucleotide position with mutation is given in parentheses.

(Fig. 2a). The *in vitro*-transcribed mutant J6/JFH1 RNAs were electroporated into Huh-7.5 cells and mutant viruses were generated. Then, naïve Huh-7.5 cells were infected with each virus at an m.o.i. of 0.01 and cultured for 12 days. The culture supernatant was collected every day from 1 to 12 days post-infection. The ability of each mutant virus to release infectious virus particles was examined by titration assay. As shown in Fig. 2(b), the recombinant viruses with single point mutations did not enhance the production of infectious virus particles, suggesting that a single point mutation is not enough for the enhanced infectivity.

Table 1. Specific-infectivity titres of the adaptive J6/JFH1 mutant viruses

Virus	HCV RNA copies [$\log_{10}$(GE ml^{-1})]	Infectivity titre [$\log_{10}$(f.f.u. ml^{-1})]	Specific infectivity (f.f.u.: GE)
P-1	6.7±0.1	4.6±0.1	1:133
P-27	7.3±0.1	6.0±0.2	1:21
P-38	7.4±0.1	6.4±0.0	1:10
P-47	7.3±0.1	6.3±0.2	1:10

Effects of combination of adaptive mutations on the production of infectious HCV

We then generated recombinant viruses with several mutations, as shown in Fig. 3(a). Naïve Huh-7.5 cells were infected with each virus at an m.o.i. of 0.01 and cultured for 12 days. The culture supernatant was collected every day from 1 to 12 days post-infection. The ability of each mutant virus to release infectious virus particles was examined by titration assay. The R-27, R-38 and R-47 viruses reached higher titres than the wild type and other mutant viruses, suggesting that all of the mutations in E2, NS2, NS5A and NS5B were important for the enhancement of infectivity (Fig. 3b). To determine the specific infectivities of the mutant viruses, the ratio of the viral infectivity titre (f.f.u. ml^{-1}) to the HCV RNA content (GE

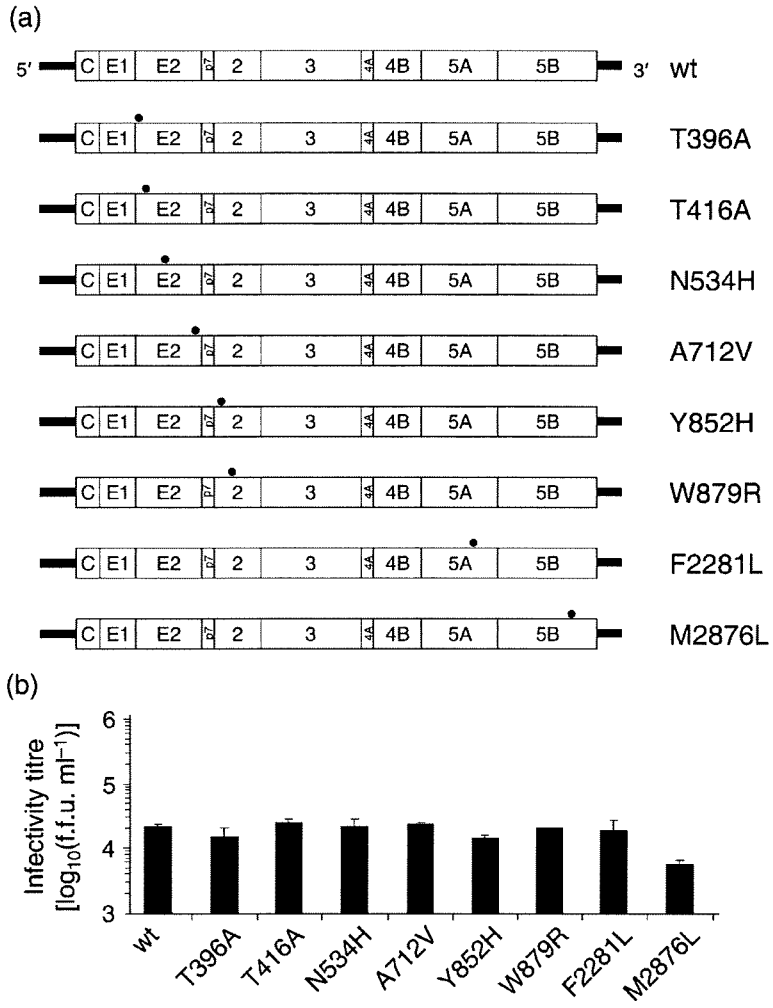

Fig. 2. Effects of individual mutations on the production of infectious HCV. (a) Schematic representation of the wild-type (wt) and mutant chimeric HCV J6/JFH1 genomes. HCV J6/JFH1 mutants with a single point mutation are shown. The adaptive mutations T396A, T416A, N534H, A712V, Y852H, W879R, F2281L and M2876L are indicated by ●. (b) The *in vitro*-transcribed mutant J6/JFH1 RNAs were electroporated into Huh-7.5 cells to generate recombinant mutant viruses. The infectivity titres of the culture supernatants were measured by titration assay. Then, naïve Huh-7.5 cells were infected with each virus at an m.o.i. of 0.01 and cultured for 12 days. The culture supernatant was collected every day from 1 to 12 days post-infection. The ability of each mutant virus to release infectious virus particles was examined by titration assay. Infectivity titres reached maximal levels at 10 days post-infection and the maximal infectivity titres were plotted. Error bars represent SD for triplicate measurements.

ml^{-1}) was calculated as shown in Table 2. The recombinant mutant viruses, R-27, R-38 and R-47, had higher specific-infectivity titres (1 : 46, 1 : 35 and 1 : 54, respectively) than the wild-type virus P-1 (1 : 197), suggesting that the particles released from cells infected with the R-27, R-38 and R-47 viruses are more infectious than those released from cells infected with the wild-type J6/JFH1 virus.

Efficient expression of HCV proteins in Huh-7.5 cells infected with the adaptive mutants

To investigate further the mechanism of adaptive mutations, we performed immunofluorescence staining of the infected cells. Huh-7.5 cells (6×10^4 cells per 24-well plate) were infected with the P-1, R-27, R-38 and R-47 viruses (1.2×10^4 f.f.u.) at an m.o.i. of 0.2. Cells were fixed 5 days post-infection and stained for immunofluorescence. Approximately 90 % of the cells were HCV-positive in the P-1-, R-27-, R-38- and R-47-infected cells (Fig. 4a). We next examined protein synthesis by immunoblotting for the HCV core and NS3 proteins. Immunoblot analysis of the cell lysates demonstrated that the levels of the core and NS3 proteins in cells infected with the R-27, R-38 and R-47 viruses were 2.0- to 2.5-fold higher than those in cells infected with the P-1 virus (Fig. 4b, c), suggesting that these mutant viruses have a replicative advantage.

Growth curves of infectious HCV after transfection of RNAs or infection with HCV

To determine whether the replicative advantage is at the level of entry or replication/translation of the genome, we examined one-step growth curves by transfecting equivalent amounts of RNAs of the wild-type and the mutant viruses into Huh-7.5 cells by means of electroporation (Fig. 5a, b). The intracellular and extracellular core protein levels were quantified by core protein-specific ELISA at the indicated times. The one-step growth curves showed that the intracellular and extracellular core protein levels increased with very similar kinetics in the cells transfected with the wild-type and adapted RNAs (Fig. 5a, b).